

AN ABSTRACT OF THE THESIS OF

JOHN WALTER LIDSTROM, Jr. for the DOCTOR OF PHILOSOPHY
(Name) (Degree)

in GEOLOGY presented on May 18, 1971
(Major) (Date)

Title: A NEW MODEL FOR THE FORMATION OF CRATER LAKE
CALDERA, OREGON

Abstract approved: Signature redacted for privacy.
Dr. E. M. Taylor

During the Pleistocene, an andesitic volcano named Mount Mazama grew to a probable elevation of 3000 meters in south-central Oregon. Near the end of the Pleistocene, three diverse magma types appeared in the eruptive products associated with Mount Mazama: 1) High-alumina basaltic andesite magma associated with an early plateau and with coeval cinder cones; 2) Hypersthene andesite magma similar in composition to the andesite which had formed the main cone; 3) Dacite magma, erupted both as pyroclastic material and as flank lava flows after formation of the andesitic cone.

Approximately 12,000-13,000 years ago, eruption of andesite and then dacite occurred along a semicircular fracture now represented by the north wall of the caldera. The eruption of dacite was a surface expression of a shallow chamber of dacite magma emplaced beneath Mount Mazama. Before and after emplacement of the dacite

magma chamber, basaltic andesite erupted upon the lower flanks and plateau surrounding the volcano. The last such parasitic activity occurred at Forgotten Crater (on the western flank of Mount Mazama) where lava and pumice of intimately mixed dacite and basaltic andesite appeared.

Approximately 6600 years ago, explosive eruption of dacite pumice began from central vents. The magma of these initial eruptions was characterized by discrete gas nuclei which expanded rapidly, disrupted the enclosing liquid into fine ash, and provided the energy to propel this ash high above the summit. As eruption proceeded, magma was tapped in which gas nuclei were actively forming and were thoroughly dispersed through the magma. At this stage, the erupted material behaved as a fluidized mass, frothed over the crater rim, and rushed down the slopes as glowing avalanches. Immediately following eruption of fluidized dacite, a more mafic magma was erupted in the form of basic scoria flows. This basic scoria was chemically similar to parasitic eruptions of basaltic andesite, and was not nearly as mobile as the earlier dacite ash-flows. The waning stages of eruption were characterized by crystal-rich basic scoria containing abundant fragments of andesite and granodiorite. Following the eruption of crystal- and lithic-rich basic scoria, the summit of Mount Mazama collapsed into the underlying magma chamber, producing the Crater Lake caldera. Soon after collapse, eruption of

mafic magma occurred on the caldera floor, probably forming a lava lake. The last eruption formed an intra-caldera andesitic cone called Wizard Island. Wizard Island lavas are chemically similar to the andesites which formed the main cone of Mount Mazama. Thus, a sequence of volcanic activity culminating in violent eruption and collapse, returned to its initial condition.

Calculations of Mazama ash volume are presented, and it is concluded that there is no discrepancy between volume of missing Mount Mazama and volume of erupted material. Crystal-rich basic scoria flows containing melted granitic fragments (torn from the margins of the dacite magma chamber) indicate that the chamber was essentially emptied during the culminating eruptions. It is suggested that basic scoria magma occupied the bottom portion of the dacite magma chamber. This mafic magma assimilated granodiorite which had crystallized around the margins of the dacite magma.

A new model for the formation of the Crater Lake caldera is presented. In this model the magma types recognized at Crater Lake ascended through the crust as independent bodies. Whenever two of these magma types came into marginal contact, limited eruption of mixed magmas was possible. However, prior to the culminating eruptions, a high-temperature, basaltic andesite magma was injected into the lower portion of the volatile-saturated, cooling dacite magma. Energy transferred from the mafic magma triggered exsolution of gas

in the silicic magma until vapor pressure exceeded confining pressure. Once eruption began, it did not stop until the chamber was depleted of its gas-rich magma. The Crater Lake caldera was formed when the unsupported summit of Mount Mazama collapsed into this sub-volcanic vacancy. Many other calderas, long recognized as a special (Krakatoan) type, were produced following the eruption of more than one magma. It is suggested that the process described above is an important caldera-forming mechanism.

A New Model for the Formation of Crater
Lake Caldera, Oregon

by

John Walter Lidstrom, Jr.

A THESIS

submitted to

Oregon State University

in partial fulfillment of
the requirements for the
degree of

Doctor of Philosophy

June 1972

APPROVED:

Signature redacted for privacy.

Associate Professor of Geology/
in charge of major

Signature redacted for privacy.

Acting Chairman of Department of Geology

Signature redacted for privacy.

Dean of Graduate School

Date thesis is presented

May 18, 1971

Typed by Mary Jo Stratton for John Walter Lidstrom, Jr.

ACKNOWLEDGEMENTS

The author wishes to express his appreciation to Dr. E. M. Taylor for his assistance and constant encouragement during the course of this study and preparation of this manuscript. Greatly appreciated are the helpful suggestions and encouragement of Drs. C. E. Wicks, H. E. Enlows, and C. W. Field who served on my committee. Special thanks are extended to Drs. M. E. Harward, J. A. Norgren, E. G. Knox, and C. T. Youngberg for their assistance on the section dealing with Mazama ash volume.

Financial support of this project by a Geological Society of America Penrose Bequest Research Grant and the Mazama Research Assistance Program, as well as cooperation and assistance by the Crater Lake National Park Service during the summers of 1968-1970 are gratefully acknowledged.

In conclusion, the author would like to thank his wife, Judith. Without her understanding, encouragement, and guidance in preparation of this manuscript, the author could not have met the requirements for this degree.

TABLE OF CONTENTS

	<u>Page</u>
INTRODUCTION	1
GEOLOGY OF MOUNT MAZAMA: A REVIEW OF PREVIOUS INVESTIGATION	4
Basement Rocks Beneath Mount Mazama	4
Main Andesite Cone of Mount Mazama	8
Early Dacites of Mount Mazama	9
Northern Arc of Vents	10
Culminating Eruptions	14
Origin of the Caldera	18
Post-Caldera Eruptions	20
Parasitic Eruptions	21
Summary of Chemical Variation	22
NEW DATA	29
Revised Estimates of Magmatic Volumes	29
Granitic Fragments Associated with the Culminating Eruptions	40
Description of the Granitic Ejecta	40
Distribution of Granitic Ejecta	43
Petrography of the Granitic Fragments	46
Chemistry of the Granitic Fragments	56
Origin and Significance of the Granitic Ejecta	61
ORIGIN OF CRATER LAKE CALDERA: A NEW MODEL	69
The Zoned Magma Chamber	70
Mechanism for Supersaturation of the Dacite Magma	72
A Summary of the Development of the Crater Lake Caldera	76
BIBLIOGRAPHY	82

LIST OF TABLES

<u>Table</u>		<u>Page</u>
1	Chemical analyses of the eruptive products associated with Mount Mazama (after Williams, 1942 and McBirney, 1968).	26
2	Thickness of Mazama ash sections.	32
3	Modal analyses of granitic ejecta associated with the culminating eruptions.	54
4	Chemical analyses of the eruptive products associated with Mount Mazama.	59

LIST OF FIGURES

<u>Figure</u>		<u>Page</u>
1	Index map.	2
2	Physiographic divisions of Western Oregon.	5
3	Geologic map of Crater Lake and vicinity.	7
4	Harker variation diagram of Crater Lake rocks.	23
5	Distribution of Mazama ash.	31
6	Mazama air-fall ash thickness along a north and northeast vector.	36
7	Directional parameters used in analytical estimation of ash volume.	37
8	Melted granitic fragment.	42
9	Distribution of granodiorite-bearing chaotic deposits of the final dying eruptions from Mount Mazama.	45
10	Cross-section of chaotic deposits containing andesite, granitic fragments, and crystal-rich basic scoria.	47
11	Photomicrograph of unmelted coarse-grained granitic fragment.	49
12	Photomicrograph of coarse-grained granitic fragment exhibiting little or no glass.	49
13	Photomicrograph of slightly melted coarse-grained granitic fragment.	51
14	Photomicrograph of melted coarse-grained granitic fragment.	51
15	Photomicrograph of intensely melted granitic fragment.	53

Figure

Page

16	Photomicrograph of fine-grained granitic fragment.	53
17	Percent granophyric texture versus increased temperature as inferred from alteration of mafic silicates and content of glass.	55
18	Harker variation diagram of Crater Lake rocks.	57
19	Temperature T at various points in an intrusive sheet.	63

A NEW MODEL FOR THE FORMATION OF CRATER LAKE CALDERA, OREGON

INTRODUCTION

In south-central Oregon (Figure 1) an andesitic volcano, which has been named Mount Mazama, grew to a probable height of 3000 meters above sea level. Approximately 6600 years ago, following violent eruptions of dacite pumice and ash, the summit of Mount Mazama collapsed. The collapse produced a caldera between 8 and 10 km across and approximately 1200 meters deep. Lava flows and cinder cones modified the floor of the caldera before it was covered by the water of present-day Crater Lake.

Mount Mazama is one of many Pleistocene volcanoes which occur in the High Cascade Range of Washington, Oregon, and northern California (Coombs, 1960). The alkali-lime index of the Cascade volcanic province ranges from 58 to 63.7, corresponding to Peacock's calc-alkalic and calcic classes (Turner and Verhoogen, 1960). The Cascade volcanic province is considered a portion of the Circum-Pacific andesite belt (Gorshkov, 1970). Of the many young calderas in this belt, Krakatoa in Indonesia and Shikotsu in Hokkaido appear to be most closely analogous to Crater Lake in form and development. A large number of additional calderas, while not exactly analogous to Crater Lake, share so many common features that a similar

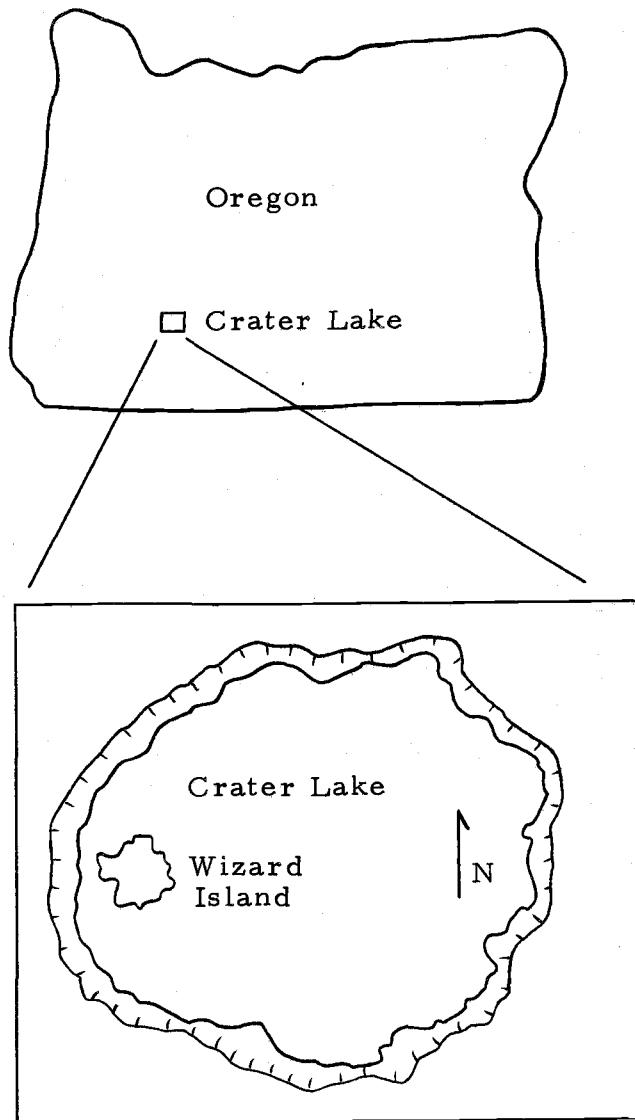


Figure 1. Index map.

mechanism might be an integral part of their development.

The scope of this investigation covers three rather broad categories. The first is a review of published works concerning formation of the Crater Lake caldera; the second is a presentation of new observations, measurements, and calculations which have a bearing on interpretation of previous work; and finally, a new model for the caldera-forming mechanism is presented.

GEOLOGY OF MOUNT MAZAMA: A REVIEW OF PREVIOUS INVESTIGATION

Since the purpose of this work is to offer new interpretations of a well-known geologic feature, a thorough review of previous investigation is necessary. The major part of this review was taken from Williams' (1942) study of Crater Lake National Park. Although many other geologists have contributed to the geology and origin of Crater Lake, principal credit for unraveling the geological events leading to caldera formation belongs to Williams.

Basement Rocks Beneath Mount Mazama

The Oregon Cascade Range is bordered on the southwest by the mountainous Klamath-Siskiyou physiographic province (Figure 2). The Klamath-Siskiyou Mountains are composed mainly of deformed pre-Tertiary strata intruded by large bodies of igneous rock ranging in character from serpentinized ultramafics to granite (Baldwin, 1964). Similar rocks are exposed in northeastern Oregon (Baldwin, 1964). Structural trends (King, 1958; Wise, 1963) and regional gravity surveys (Blank, 1966) indicate that this pre-Tertiary igneous and metamorphic complex very likely extends beneath the Cascades of southern and central Oregon. However, no fragments of this rather distinctive basement complex have been reported in the ejecta of Mount Mazama.

From Late Eocene to Late Miocene, volcanism was widespread

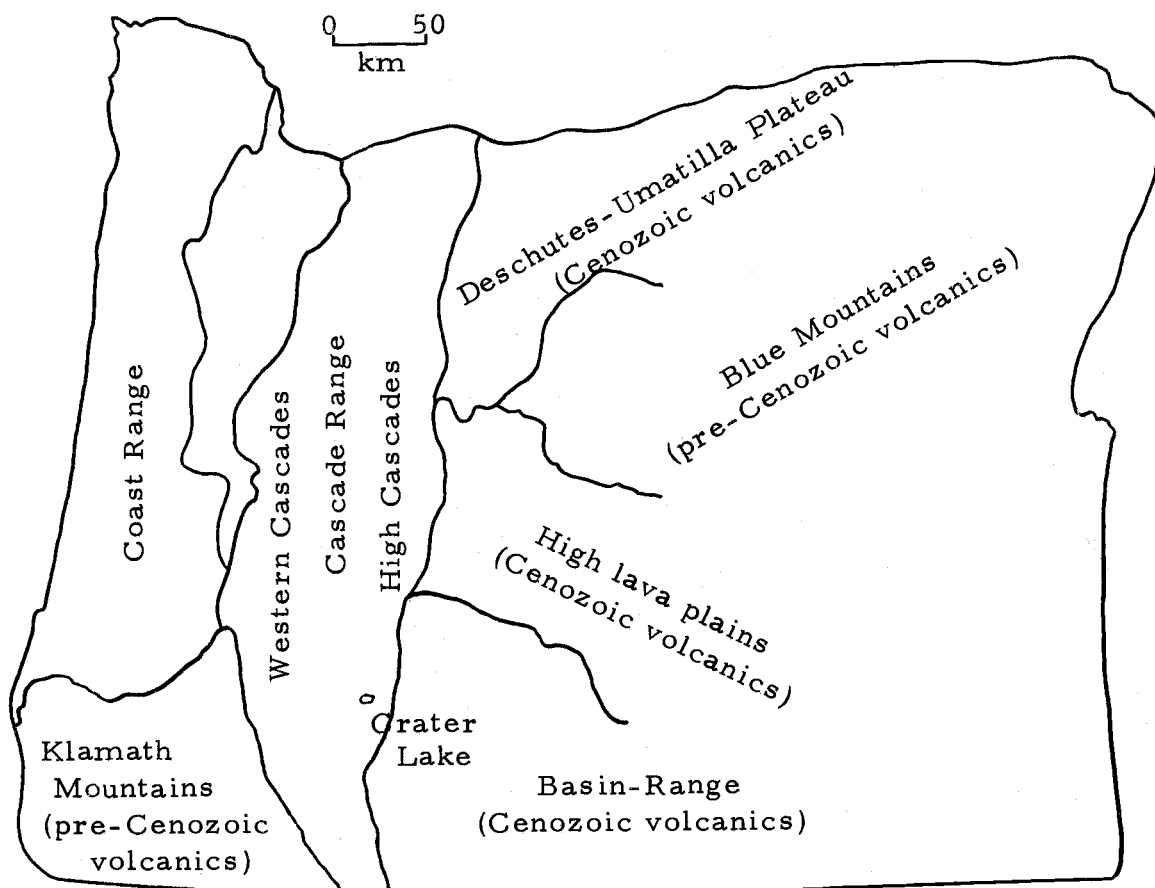
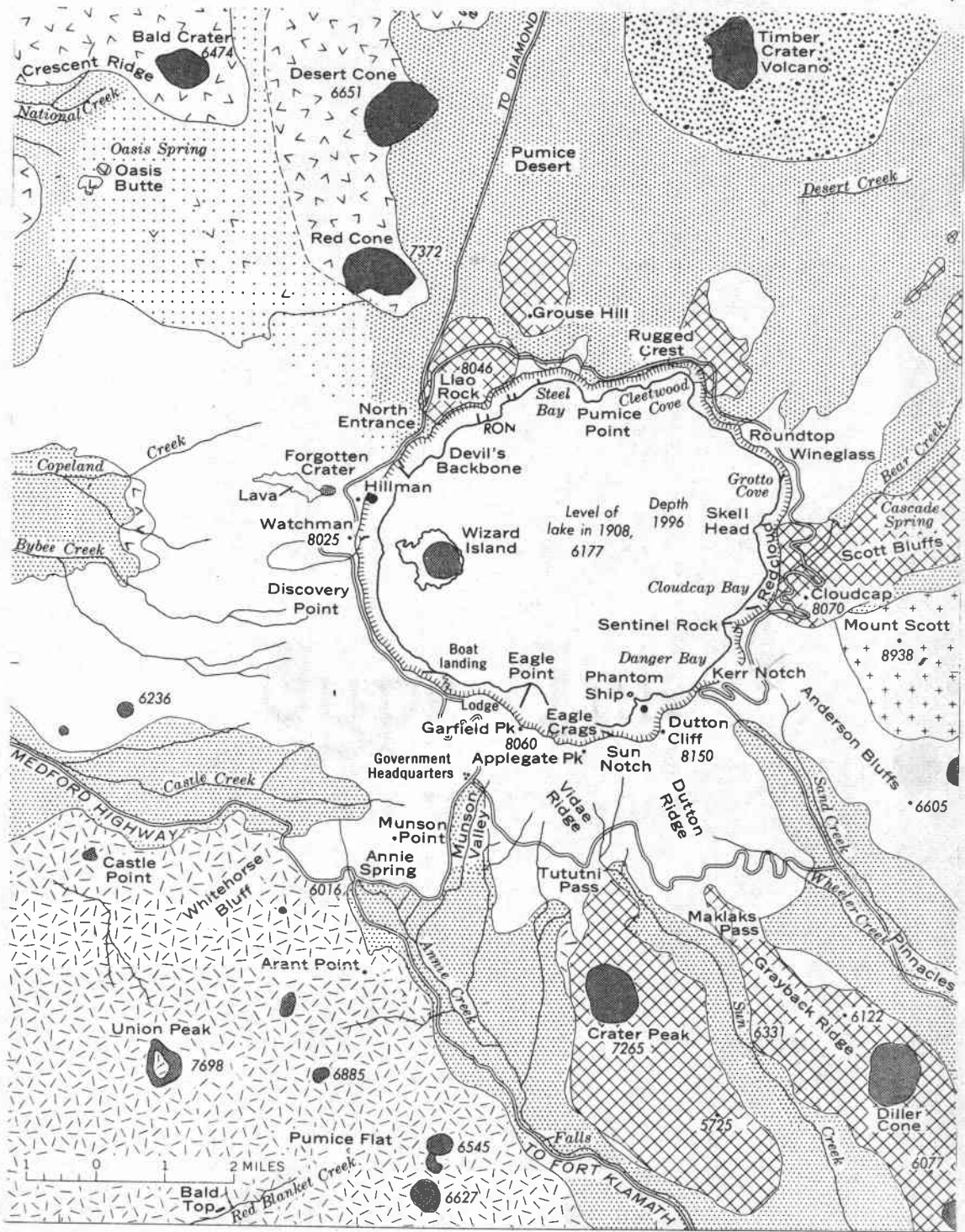


Figure 2. Physiographic divisions of Western Oregon. (After Baldwin, 1964)

along the north-south physiographic province of the Western Cascades (Peck et al., 1964) (Figure 2). Deformed and partially altered flows and pyroclastic rocks of this province interfinger with or overlie marine sedimentary rocks to the west. These calc-alkalic volcanics range from basalt to rhyolite with the average composition being silicic andesite or dacite (Peck et al., 1964).

During the Pliocene, deformed and deeply eroded rocks of the Western Cascades were partially buried by volcanic products of the High Cascades (Figure 2). The volcanoes which formed the High Cascades were less explosive than those which formed the Western Cascades (Williams, 1942), and by the end of the Pliocene, the site of the High Cascades had become a plateau formed by coalescence of broad shield volcanoes of mafic lava chemically similar to the mafic lavas of the Western Cascades. Some of these shield volcanoes were surmounted by large summit cones. Union Peak, 12 km southwest of Mount Mazama (Figure 3), is a glacially dissected example, and a volcano named Phantom Cone, buried beneath Mount Mazama, is probably of similar origin.

In summary, the basement beneath Mount Mazama can be separated into three distinct units. The oldest unit is probably similar to the igneous and metamorphic rocks exposed in the Klamath-Siskiyou Mountains. Overlying the oldest unit, one would expect to find deformed and altered volcanic rocks similar to those exposed in the



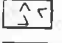
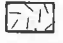


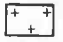
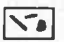



- | | | |
|--|--|--|
|  Pre-Mazama Lavas |  Union Peak Lavas |  Mount Mazama Andesites |
|  Mount Mazama Dacites |  Mount Scott Lavas |  Dikes and vents on caldera walls |
|  Parasitic cinder cones |  Glowing avalanche deposits |  Timber Crater Lavas |

Figure 3. Geologic map of Crater Lake and vicinity (after Williams, 1942).

Western Cascade Range, and finally, directly beneath Mount Mazama are the basaltic andesite shield volcanoes of the High Cascade Range.

Main Andesite Cone of Mount Mazama

In the Pleistocene, andesitic volcanoes began to develop on the earlier plateau of shield volcanoes. Mount Mazama was one of these andesitic cones which continued to develop into Recent times. The main cone of Mount Mazama was built by quiet effusions of hypersthene andesite upon the basaltic andesite shields. The plateau reached an elevation between 1500 and 1800 meters and the summit of Mount Mazama probably reached a maximum elevation of 3000 meters (Williams and Goles, 1968).

Mazama andesite flows generally range in thickness from 3 to 25 meters. Flows which issued from summit vents are decidedly thinner than flows which appear to have issued from flank vents. Columnar jointing is rare, but platy jointing both parallel and perpendicular to flow planes is common.

The andesites range from black to pale-gray depending upon the amount of glass present. Where fumarolic gases have been active, colors range from pale-brown to pink or even dark brick-red. Although the andesites differ markedly in color and hand-specimen appearance, they are texturally and mineralogically uniform in thin section. They range from holocrystalline and subophitic to glass-rich, with

pilotaxitic texture commonly developed. Plagioclase phenocrysts are generally zoned, ranging in composition from labradorite to andesine. Ferromagnesian phenocrysts are usually subordinate (both in size and abundance) to plagioclase. Hypersthene may comprise ten percent of the rock, but usually is less than five. Occasionally, phenocrysts of augite may be the predominant ferromagnesian mineral. In pilotaxitic andesites the matrix consists generally of microlites of oligoclase and sodic andesine or both, and anhedral grains of augite and magnetite. Olivine is an unusual accessory among the hypersthene andesites. Rare crystals of hornblende rimmed by magnetite are present.

Many of the andesite flows contain crystalline inclusions. In places the inclusions comprise one-quarter of the total volume, and presumably represent solidified magma torn from the walls of the conduits or margins of the underlying magma chamber. The inclusions consist of a crisscross felt of slender plagioclase laths, prisms of hypersthene and augite, and magnetite with interstitial brown glass, cristobalite, and tridymite. No fragments of metamorphic or granitic rocks have been recognized as inclusions in the andesites.

Early Dacites of Mount Mazama

After the main andesitic cone of Mount Mazama formed, flows of dacite broke out along fissures far down the south flank. The resulting lava now occupies the crests of Vidae and Grayback ridges (Figure 3).

After extrusion, these dacitic flank lavas were almost completely buried by glaciers overflowing the valleys of Sun, Sand, and Annie creeks.

Zoned phenocrysts of plagioclase, commonly corroded and containing abundant glass inclusions, are plentiful in the dacite lavas. Generally, the zoning is from labradorite in the center to oligoclase at the margins. Hypersthene and augite (hypersthene usually predominating) often show discoloration and marginal separation of magnetite. Perlitic fractures indicate that glass was once abundant in the lavas, but now is devitrified to microfelsite and microlites of oligoclase and sodic andesine. Phenocrysts comprise between 10 and 20 percent of these early dacite lavas.

Dacite pumice, including several deposits of welded tuff, is found underlying andesitic lavas in the eastern caldera wall, and was probably erupted from central vents during flank eruptions of dacite lava. Presumably, these pumice deposits belong to a period of transition in Mazama's history, in which eruption of andesitic magma gave way to dacite flows and other products of the culminating eruptions (Williams, 1942).

Northern Arc of Vents

After extrusion of the early dacites, a northern arc of eruptive centers became active. Williams (1942) refers to these eruptions as

the Northern Arc of Vents, and suggests they represent a surface expression of enlargement of the underlying magma chamber.

Six vents of this northern arc are visible on the caldera wall. The middle three vents produced Llao Rock, Cleetwood, and Redcloud dacite flows (Figure 3). These dacites are flanked on the west by the Hillman Peak and Watchman andesites, and on the east by andesite of Sentinel Rock. The exact order of eruption has not been positively established; however, andesite vents were active before those which erupted dacite.

The Hillman parasitic cone was built first by explosions of viscous scoria, and later by flows of porphyritic andesite. The flows were confined to the immediate vicinity of the cone, and activity probably ceased before eruption from the Watchman and Sentinel Rock vents.

The Watchman flow of pale-gray porphyritic andesite is between 120 and 150 meters thick. The viscosity of the flow must have been high, for the snout and sides of the flow are extremely steep. It is one of the youngest pre-caldera andesites and probably contemporaneous with the Sentinel Rock andesite.

The Sentinel Rock andesite flow varies between 90 and 120 meters in thickness, and is characterized by abundant crystalline inclusions. Locally, these inclusions comprise as much as one-quarter of the total volume, and suggest extensive crystallization along the conduit walls.

Eruption of the Llao Rock dacite was preceded by explosions which deposited dacite pumice around the vent. The flow was erupted into a U-shaped glacial valley and reaches a maximum thickness of 365 meters. The bulk of the flow consists of streaky glass which is extremely vesicular and locally pumiceous. The chief minerals present are plagioclase, augite, and hypersthene, with accessory hornblende, apatite, and magnetite. Plagioclase exhibits oscillatory zoning ranging from sodic andesine to sodic labradorite. Crystals comprise approximately 15 percent of the Llao Rock dacite.

The interior of the Cleetwood dacite flow is pale-gray and locally pumiceous, but the top and bottom consist of black obsidian. The flow appears to have been exceptionally viscous and reaches an average thickness of 100 meters. Plagioclase phenocrysts are common, hypersthene and red-brown hornblende are usually present, and augite is either absent or present as microlites. The total volume of crystals does not appear to exceed ten percent.

The Redcloud lava appears to have issued from a funnel-shaped explosion vent which is now exposed in the caldera wall. Although the bulk of Redcloud dacite is composed of clear, colorless glass, phenocrysts of zoned andesine-labradorite, hornblende, hypersthene, and augite locally comprise ten percent of the volume.

Grouse Hill is a dome-shaped dacite flow located just north of the caldera rim. The dome reaches a maximum thickness of 250-300

meters, and the vent appears to lie beneath the center of the dome. The lava is pale-gray, vitrophyric dacite characterized by fluidal banding and platy jointing. Phenocrysts of corroded and glass-charged plagioclase (zoned from labradorite to andesine), brownish-green hornblende, augite, hypersthene, and magnetite locally comprise 20-30 percent of the volume.

Presumably, the last activity from the Northern Arc of Vents is represented by the Wineglass welded tuff section, which is preserved on the north and northeast rim of the caldera. This section is composed of a thick layer of coarse lump pumice (containing abundant lithic fragments) overlain by a discontinuous unit of dacite welded tuff. The Wineglass welded tuff contains approximately 25 percent phenocrysts of zoned and corroded plagioclase with subordinate augite and hypersthene.

Although the exact age of the Northern Arc lavas and ejecta is not available, they appear to have been erupted after the last maximum glaciation of Mount Mazama. The lack of evidence for eruption onto or beneath ice indicates these vents were active during an interstade of the final glaciation. After eruption from the Northern Arc had ceased, glaciers covered all but the tops of Watchman, Hillman Peak, Llao Rock, Cleetwood, and Redcloud lava flows. Striations and patches of glacial till can be found on the Wineglass welded tuff. This final advance of ice appears to have descended only a short distance

beyond the present caldera rim (Williams, 1942).

Due to similar climate and geographic proximity, this last major episode of glaciation at Mount Mazama is probably best correlated with Frazer Glaciation in northern Washington (Easterbrook, 1969). The last major advance of Mazama ice would correspond to the Vashon stade approximately 13,000-18,000 years ago. Eruption along the Northern Arc could have occurred during the Everson interstade approximately 11,000-13,000 year ago. Finally, the last advance of ice would correspond to the Sumas stade which ended approximately 10,000 years ago. Thus, until more sophisticated dating is available, the Northern Arc eruptions are considered to have ceased approximately 12,000 years ago.

Culminating Eruptions

Approximately 6600 years ago (Rubin and Alexander, 1960), activity returned to the summit vents. The first explosions began with ejection of finely divided dacite pumice, which was thrown high above the summit and carried afar by the winds. Generally, the Mazama pumice deposits become coarser from the bottom upward, and Youngberg and Dyrness (1964) and Chichester (1967) have recognized a sharp boundary between fine and coarse particle size. Since no signs of erosion or interbedded soil have been noted within the pumice fall, the whole eruptive sequence is pictured as short-lived

with explosions following each other at brief intervals.

Crystals of plagioclase and hypersthene, with minor augite and hornblende, comprise approximately 10-15 percent by volume of the air-fall pumice. In addition to glass and crystals, the air-fall deposit contains fragments of old lava torn from conduit walls beneath and within Mount Mazama. These fragments are composed almost entirely of andesite with some dacite. Fragments torn from pre-Mazama basement rocks are extremely rare. The content of lithic fragments in the pumice fall is between three and four percent, being slightly higher in the lower part of the deposit.

As the eruption progressed, material was no longer thrown high above the vent, but frothed over the crater rim and rushed down the slopes as glowing avalanches. The extreme mobility of these ash-flows enabled them to travel 40-50 km from the summit, and distribution was influenced by pre-existing topography (Figure 3). The ash-flow deposits contain subrounded pumice lumps and lithic fragments (andesite and dacite) in a fine, dusty matrix.

Both mineralogically and chemically, the dacite ash-flow and air-fall deposits are almost identical to the dacite lavas erupted earlier from the Northern Arc of Vents. The pumice is highly vesicular, often fibrous with scattered crystals of plagioclase, pyroxene, and hornblende. The crystal content varies significantly, the average lying between 10 and 15 percent by volume. Before vesiculation

crystals may have comprised 25-30 percent of the magma, which is 10-15 percent greater than the earlier dacite lavas. Few of the crystals are larger than 2 mm and few smaller than 0.2 mm in length with the majority between 0.5 and 1 mm in length. Plagioclase is the most abundant mineral, usually more plentiful than all ferromagnesian minerals combined. Most of the feldspars exhibit oscillatory zoning ranging from labradorite to oligoclase. Glassy inclusions, often giving the feldspars a spongy appearance, are more plentiful than in feldspars of the dacite lavas. Hypersthene is generally the chief ferromagnesian mineral, but may be exceeded by augite and rarely hornblende. Resorption of hornblende and resultant formation of magnetite rims has not been observed.

Near the end of eruption, the pumice flows were followed by glowing avalanches of smoke-gray basic scoria. Basic scoria flows did not travel as far as earlier dacite pumice flows, seldom exceeding a distance of 8-10 km from the summit. The transition between the two deposits is sharp and no intermediate andesitic ejecta has been described (McBirney, 1968). When basic scoria flowed down canyons it was restricted to central troughs plowed up in earlier dacite pumice. Scoria deposits contain crystal-rich bombs and lithic fragments in a finer matrix of ash. There is no evidence of sorting or stratification, but columnar structure caused by incipient welding and contraction is often well-developed.

The basic scoria is characterized by dark-brown vesicular glass, and more plentiful crystals than the earlier dacites. The crystals include intensely zoned plagioclase ranging in composition from andesine to bytownite, hornblende (occasionally with cores of fresh olivine), augite, hypersthene, olivine, and magnetite (Diller and Patton, 1902). Relative proportions and overall abundance of crystals vary widely (Noble, 1969). Although the mineral content is different, the chemical composition of the basic scoria is very similar to that of the pre-Mazama basaltic andesite.

Lithic fragments in the combined pumice and scoria flows average approximately 15-20 percent, being higher in the scoria than in the pumice. Except for a few fragments of propylitized lava similar in appearance to some Western Cascade rocks, Williams (1942) states that all the lithic fragments contained in the basic scoria were derived from the Pliocene basement beneath Mount Mazama or from the volcano itself.

In general, the chief mineralogical differences between the basic scoria and the preceding dacite pumice are:

- 1) The basic scoria has a much greater content of ferromagnesian minerals (particularly hornblende).
- 2) The basic scoria contains olivine whereas the dacite pumice contains none.
- 3) The basic scoria contains medium bytownite - andesine

plagioclase whereas the dacite pumice contains sodic labradorite - oligoclase.

- 4) The basic scoria contains dark-brown glass whereas the dacite pumice contains light-colored glass.
- 5) The relative proportions and overall abundance of crystals is much greater and more variable in the basic scoria.

Probably the last scoria flows were deposited in the Pumice Desert, and consisted essentially of hornblende, plagioclase, accessory pyroxene, and subordinate glass. Williams (1942) suggests that these crystal-rich deposits represent deep-seated portions of the magma chamber tapped during the close of the eruptive episode. After expulsion of these crystal-rich scoria flows, most of the energy of the eruption was exhausted. However, enough gas remained to cause a sequence of dying explosions. The ejecta from these final explosions is much finer-grained, better sorted, and richer in both lithic fragments and crystals than the earlier pumice fall. Much of this latest ejecta fell near the present caldera rim and is composed of dark-brown and reddish crystal-rich scoria and small fragments of old lava.

Origin of the Caldera

The caldera of Mount Mazama is generally believed to have formed by collapse of the summit shortly after the sequence of dacite pumice and basic scoria eruptions. Several important conclusions

bearing upon the origin of the Crater Lake caldera are here summarized from Williams' early (1942) studies:

- 1) The volume of rock which has disappeared from Mount Mazama is 71 km^3 .
- 2) Only $4-8 \text{ km}^3$ were removed in the form of lithic fragments. Therefore, explosive shattering of the summit was not responsible for formation of the caldera.
- 3) The magmatic volume of pumice, scoria, and crystals produced by the culminating eruptions is approximately 21 km^3 .
- 4) If the caldera was formed by collapse of the summit because of withdrawal of magmatic support from below, the volume of the collapsed mountain should closely match the volume of withdrawn magma. Therefore, approximately 44 km^3 of magma must have been withdrawn from beneath Mount Mazama by some non-eruptive process.
- 5) Prior to caldera formation, the underlying magma chamber lay at shallow depth and a semicircular fracture had already formed on the northern flank of the volcano.
- 6) Collapse was eccentric with respect to the summit of the volcano.
- 7) Collapse appears to have been as cataclysmic as that of Krakatoa, and probably occurred in several gigantic steps.

Williams and Goles (1968) have re-calculated Williams' earlier

estimates of ash-fall volume and volume of Mount Mazama which disappeared. They reach the following conclusions:

- 1) Approximately 62 km^3 of material are missing from Mount Mazama instead of the earlier estimate of 71 km^3 .
- 2) The volume of lithic fragments ejected is $4-8 \text{ km}^3$ (unchanged from Williams' early estimate).
- 3) The total volume of magma (including crystals) was 36 km^3 instead of 21 km^3 .
- 4) A discrepancy of 20 km^3 still exists between the volume of erupted material and the volume of Mount Mazama which disappeared due to engulfment. Williams and Goles (1968) suggest that

For lack of a better explanation, some of the space necessary to permit collapse was provided by subterranean withdrawal of magma, either through fissures in the walls of the reservoir or by recession at greater depths (p. 41).

They additionally suggest that subterranean withdrawal may itself have triggered the explosive eruptions that led to engulfment.

Post-Caldera Eruptions

Probably shortly after collapse of the summit, eruption of mafic magma began on the floor of the caldera. A lava lake may have occupied the deepest part of the floor, and at least two andesitic cinder

cones and one dacite dome were formed inside the caldera (Williams, 1961). The most recent and accessible product of the intra-caldera eruptions is represented by Wizard Island. Wizard Island is a symmetrical cinder cone surrounded by dark, rugged flows of lava. The lavas of Wizard Island are hyalopilitic, hypersthene-augite andesites with accessory olivine. In most of the flows, there are sporadic inclusions consisting of unaltered xenoliths of andesite and basalt, and occasionally, vitrified inclusions of granitic material. These vitrified inclusions may be accompanied by pale-gray inclusions of dioritic appearance. According to Williams (1942) these coarsely crystalline inclusions probably represent fragments torn from the margins of the underlying magma chamber. The vitrified, pumiceous inclusions may be the result of partial melting of the coarse crystalline fragments. Williams (1942, p. 143) states

Patton has described somewhat similar rocks among the ejecta of the culminating eruptions of Mount Mazama, under the title "light-colored granophyric secretions." These are the only rocks in the Crater Lake region which are known to contain biotite.

Parasitic Eruptions

Shortly after the close of the Pleistocene, numerous cinder cones were formed near the base and on the plateau surrounding Mount Mazama. Within Crater Lake National Park there are 13 of these parasitic cones (Figure 3), of which only two small ones have been

modified by glacial action (Williams, 1942). Most of the parasitic cones were formed primarily by eruption of scoriaceous bombs and lapilli, and some erupted short flows. However, Timber Crater (Figure 3) is actually a shield volcano capped by pyroclastic cones. In general, lava and scoria of these parasitic eruptions contain phenocrysts of plagioclase and olivine, granular augite, and glass with hypersthene and magnetite as accessories.

The parasitic cone nearest to the caldera rim is Forgotten Crater. This cone was built on a ridge of lava that descends from Hillman Peak and may lie on a radial fissure connected with the Hillman Peak vent. Banded and mixed pumice similar to that of Lassen Peak (Macdonald and Katsura, 1965) was erupted. After explosive activity at Forgotten Crater had ceased, composite flows of banded pumiceous lava broke through the south side of the crater wall. The banding is composed of dark, mafic lava and paler, more silicic material. Williams (1942) suggests that this flow represents the last activity on the outer slopes of Mount Mazama before the climactic eruptions of pumice and scoria which led to collapse of the summit.

Summary of Chemical Variation

Figure 4 is a Harker diagram showing major element variation of the eruptive products associated with Mount Mazama. The analytical data are from Williams (1942) and McBirney (1968), and have been

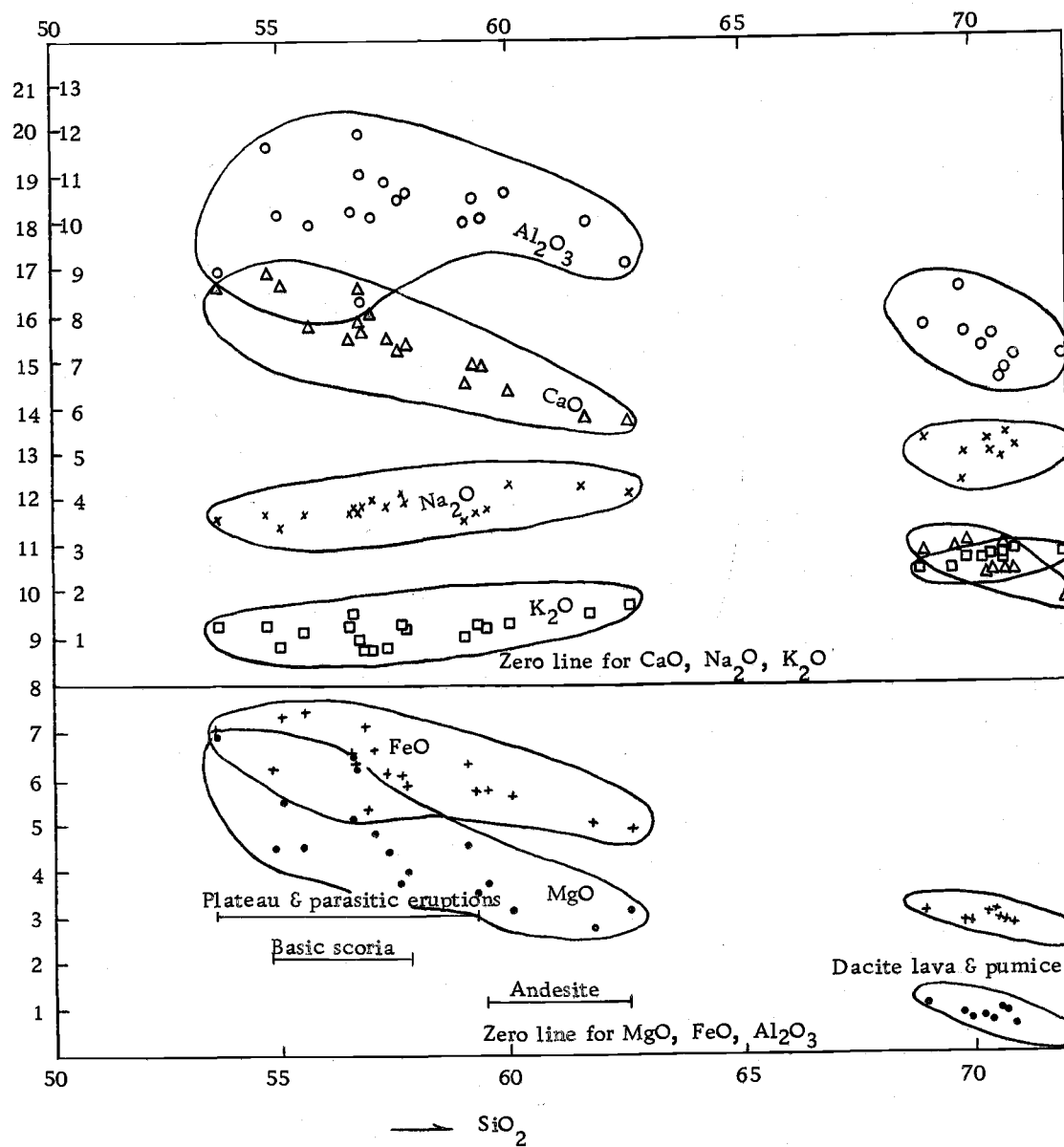


Figure 4. Harker variation diagram of Crater Lake rocks. Analyses from Williams (1942) and McBirney (1968).

recalculated water-free with total iron reported as FeO to permit direct comparison with new analyses presented in a later section. Mazama rocks have an alkali-lime index of 61-62, and would be classified as calcic (Peacock, 1931). According to Kuno (1960) the mafic members of this volcanic suite would be classified as high-alumina basalt. Following Coats (1968), the plateau and parasitic lavas as well as the basic scoria can be classified as basaltic andesite. The composite term, high-alumina basaltic andesite is used here. High-alumina basaltic andesite (Figure 4) ranges in SiO_2 content from 54.4 to 59.2 percent, and contains phenocrysts of olivine. Mazama andesite ranges in SiO_2 content from 59.4 to 62.5 percent, and does not contain phenocrysts of olivine. High-alumina basaltic andesite formed shield volcanoes and cinder cones throughout the region, while andesite was restricted to eruption from vents associated with Mount Mazama. There is no sharp chemical discontinuity between the high-alumina basaltic andesite and andesite analyses. Mazama dacite ranges in SiO_2 content from 68.8 to 72.3 percent, and is restricted to the vicinity of the andesite cone. There is a distinct chemical hiatus corresponding to approximately six percent SiO_2 between the andesite and dacite analyses.

While the magmas associated with Mount Mazama may have been closely related at their depth of formation, three magma types appear to be represented at the surface. The first magma was a high-alumina

basaltic andesite, discontinuously produced over a wide area before, during, and after formation of Mount Mazama in the form of basement plateaus, parasitic cones, and intra-caldera lavas. The second magma to appear was andesite which formed the main cone of Mount Mazama. The third magma was dacite which made its first appearance after the main cone of Mount Mazama had developed. The chamber which fed the culminating eruptions just prior to collapse contained two distinct magmas. The upper and more voluminous magma was dacite, chemically equivalent to eruptions of dacite lava along the Northern Arc, while the lower magma was chemically similar to coeval parasitic eruptions of high-alumina basaltic andesite. There was no hiatus in the eruptive history and no intermediate material erupted from this zoned magma chamber.

1. Hypersthene-bearing olivine basalt. Southwest base of Red Cone (Williams, 1942).
 2. Hornblende-rich scoria bomb. Castle Creek (Williams, 1942).
 3. Olivine basalt. North base of Union Peak (Williams, 1942).
 4. Olivine basaltic andesite. Red Blanket Canyon (Williams, 1942).
 5. Basaltic andesite, near summit of Crater Peak (Williams, 1942).
-
6. Olivine-bearing basaltic andesite. Main flow from west base of Forgotten Crater (Williams, 1942).
 7. Hornblende scoria. Pinnacles (McBirney, 1968).
 8. Scoria bomb. Sun Creek (Williams, 1942).
 9. Olivine micronorite. Union Peak (Williams, 1942).
 10. Hypersthene-bearing basaltic andesite. Annie Creek (Williams, 1942).

Table 1. Chemical analyses of the eruptive products associated with Mount Mazama (after Williams, 1942 and McBirney, 1968).^a

	<u>1</u>	<u>2</u>	<u>3</u>	<u>4</u>	<u>5</u>
SiO ₂	53.72	54.80	55.05	55.76	56.57
Al ₂ O ₃	16.90	19.71	18.2	17.96	18.24
FeO	7.05	6.20	7.29	7.40	6.52
CaO	8.57	8.86	8.62	7.75	7.50
MgO	7.03	4.47	5.45	4.49	5.18
Na ₂ O	3.58	3.72	3.41	3.74	3.69
K ₂ O	1.30	1.26	0.80	1.14	1.24
TiO ₂	1.18	0.76	0.82	1.23	0.85
Other	0.63	0.17	0.33	0.51	0.19
Totals	99.96	99.95	99.97	99.98	99.98
	<u>6</u>	<u>7</u>	<u>8</u>	<u>9</u>	<u>10</u>
SiO ₂	56.76	56.79	56.80	57.00	57.30
Al ₂ O ₃	16.27	19.96	19.07	18.13	18.93
FeO	6.35	5.32	7.16	6.60	6.15
CaO	7.84	8.29	7.60	8.00	7.47
MgO	6.20	3.80	3.60	4.80	4.38
Na ₂ O	3.80	3.84	3.90	4.05	3.90
K ₂ O	1.55	0.99	0.71	0.71	0.82
TiO ₂	0.94	0.76	0.77	0.56	0.79
Other	0.28	0.22	0.36	0.18	0.23
Totals	99.99	99.97	99.97	100.03	99.97

(Continued on next page)

11. Hornblende scoria. Pinnacles (McBirney, 1968).
12. Hornblende-rich scoria bomb. Liao Rock (Williams, 1942).
13. Olivine-bearing basaltic andesite. Timber Crater (Williams, 1942).
14. Hypersthene-bearing basaltic andesite. Desert Ridge (Williams, 1942).
15. Hypersthene andesite flow. Lake level under Liao Rock (Williams, 1942).

16. Hypersthene andesite. Wizard Island (Williams, 1942).
17. Hypersthene andesite. Rim just south of Watchman (Williams, 1942).
18. Hypersthene andesite. Palisades (Williams, 1942).
19. Welded dacite tuff. Wineglass (Williams, 1942).
20. Dacite lump pumice. Sun Creek (Williams, 1942).
21. Dacite pumice. Pinnacles (McBirney, 1968).

Table 1. (Continued)

	<u>11</u>	<u>12</u>	<u>13</u>	<u>14</u>	<u>15</u>	
SiO ₂	57.60	57.72	59.00	59.20	59.40	
Al ₂ O ₃	18.55	18.60	18.00	18.55	18.14	
FeO	6.05	5.83	6.32	5.66	5.78	
CaO	7.20	7.31	6.47	6.97	6.92	
MgO	3.73	3.98	4.50	3.50	3.66	
Na ₂ O	4.20	3.95	3.57	3.71	3.83	
K ₂ O	1.30	1.24	1.01	1.32	1.25	
TiO ₂	1.05	1.10	0.80	0.81	1.25	
Other	0.38	0.26	0.29	0.23	0.27	
Totals	<u>99.96</u>	<u>99.99</u>	<u>99.95</u>	<u>99.95</u>	<u>99.97</u>	
	<u>16</u>	<u>17</u>	<u>18</u>	<u>19</u>	<u>20</u>	<u>21</u>
SiO ₂	59.95	61.67	62.50	68.91	69.69	69.82
Al ₂ O ₃	18.62	18.02	17.10	15.77	16.52	15.50
FeO	5.56	5.05	4.87	3.03	2.83	2.83
CaO	6.35	5.79	5.70	2.79	2.81	3.00
MgO	3.15	2.70	3.10	1.02	0.78	0.61
Na ₂ O	4.32	4.30	4.13	5.20	4.30	4.88
K ₂ O	1.30	1.45	1.68	2.48	2.48	2.65
TiO ₂	0.42	0.72	0.65	0.54	0.50	0.57
Other	0.31	0.28	0.33	0.22	0.05	0.12
Totals	<u>99.98</u>	<u>99.98</u>	<u>100.03</u>	<u>99.96</u>	<u>99.96</u>	<u>99.97</u>

(Continued on next page)

22. Hypersthene dacite. Cleetwood flow (Williams, 1942).
23. Dacite pumice. Pinnacles (McBirney, 1968).
24. Dacite lava. Grouse Hill (Williams, 1942).
25. Dacite lump pumice. Chemult (Williams, 1942).
26. Dacite pumice. Pinnacles (McBirney, 1968).
27. Dacite pumice. Pinnacles (McBirney, 1968).

Table 1. (Continued)

	<u>22</u>	<u>23</u>	<u>24</u>	<u>25</u>	<u>26</u>	<u>27</u>
SiO ₂	70.22	70.37	70.56	70.6	70.80	72.14
Al ₂ O ₃	15.25	15.26	14.57	14.65	15.05	15.08
FeO	3.0	3.01	2.90	2.85	2.67	2.45
CaO	2.30	2.34	2.95	2.42	2.40	1.67
MgO	0.75	0.61	0.93	0.85	0.55	0.28
Na ₂ O	5.20	4.94	4.88	5.33	5.07	5.07
K ₂ O	2.62	2.68	2.68	2.54	2.77	2.72
TiO ₂	0.48	0.58	0.44	0.59	0.54	0.48
Other	0.23	0.18	0.09	0.13	0.12	0.09
Totals	100.05	99.97	100.00	99.96	99.97	99.98

^aAll analyses have been converted to a water-free state. All Fe₂O₃ has been converted to FeO.

NEW DATA

Revised Estimates of Magmatic Volumes

The caldera at Crater Lake was produced by collapse of the summit resulting from rapid removal of magma from a high-level magma chamber (probably less than 10-15 km beneath Mount Mazama). The volume of material removed from this chamber should therefore closely approximate the volume of Mount Mazama which collapsed. Williams and Goles (1968) estimate that approximately 62 km^3 of Mount Mazama disappeared due to engulfment. They can account for only 42 km^3 of erupted material surrounding Crater Lake. Therefore, a discrepancy of approximately 20 km^3 exists between the volume of Mount Mazama which disappeared and the volume of erupted material. Williams and Goles (1968) suggest that withdrawal of a portion of the magma at depth may be responsible for this discrepancy.

A compilation of data on calderas (Williams and McBirney, 1968) indicates that Crater Lake is the only known Krakatoan type of caldera exhibiting a discrepancy between volume of erupted material and volume of collapse. At Shikotsu caldera in Hokkaido, and Coatepeque caldera in El Salvador, the volume of erupted material can be accurately calculated and no discrepancy is found. Thickness estimates for Mazama ash in bog sites and upland soils of north-eastern Oregon (Harward and Youngberg, 1969; Rai, 1971) are in

excess of that predicted from the curve presented by Williams and Goles (1968). This indicates that Williams and Goles' (1968) calculation of air-fall ash volume is underestimated, and a re-evaluation of this volume is necessary.

Thickness of pumice deposits within 100 km of Crater Lake (Harward, Youngberg and Knox, personal communication)¹ is consistent with the isopach map of Mazama pumice presented by Williams (1942). Therefore, Williams' (1942) estimate of 27 km³ (magmatic volume) appears to be accurate for the erupted material within 100 km of Crater Lake. Williams and Goles (1968) showed that a considerable volume of ash fell beyond 100 km of Crater Lake. It is evident (Williams, 1942) that the major lobe of air-fall ash is found along a northeasterly trend from the source. Thickness of ash in the Ochoco and Blue Mountains of Oregon is also consistent with the presence of a northeastern lobe (Harward and Youngberg, 1969; Rai, 1971). However, Williams and Goles (1968) attempted to estimate the volume of ash by using a thickness distribution along a northerly trend. They set up an equation for the differential volume in an arcuate segment, and using a northerly thickness distribution, integrated over distances from Crater Lake within the area known to contain Mazama ash. Recent data (Figure 5) have not only expanded the area known to

¹ Unpublished data. Soils Department, Oregon State University, Corvallis.

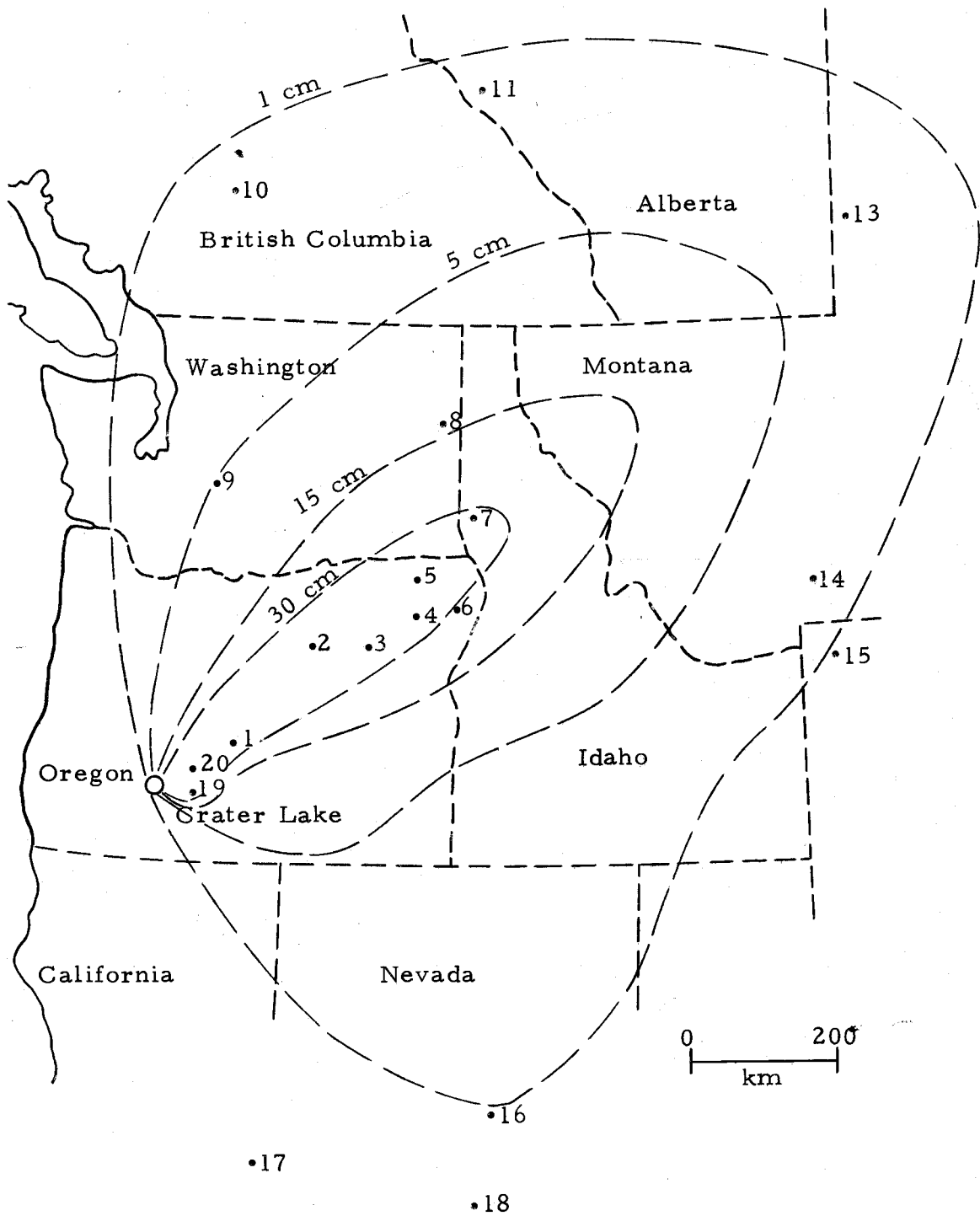


Figure 5. Distribution of Mazama Ash. Isopachs present a thickness distribution of ash with an average bulk density of 0.7 g/cc.

Table 2. Thickness of Mazama ash sections.

Location	Description
1	South Ice Cave (Harward and Youngberg, 1969), 68 cm upland thickness.
2	Simpson Place Bog (Harward and Youngberg, 1969) ¹ , 30 cm bog thickness converted to 60 cm upland.
3	Day Creek (Rai, 1971), 47 cm upland thickness.
4	Anthony Lake Meadow (Harward and Youngberg, 1969) ¹ , 18 cm bog thickness converted to 36 cm upland.
5	Tollgate Pass Bog (Rai, 1971), 18.5 cm bog thickness converted to 37 cm upland.
6	Hurricane Creek (Harward and Youngberg, 1969) ¹ , 12.5 cm bog thickness converted to 25 cm upland.
7	Moscow (Garber, 1970), 60 cm upland with overthickening present. Original thickness is considered to be approximately 30 cm.
8	Newman Lake (H. Hansen, personal communication), no exact measurements are yet available, however a thick section is present (perhaps 15-30 cm).
9	Mount Rainier (Crandell and Mullineaux, 1967), 5 cm upland ash.
10	Jesmond Bog (Williams and Goles, 1968), 5 mm bog thickness converted to 1 cm upland.
11	Banff (Westgate and Dreimanis, 1967), no thickness available.
12	Lofty Lake (Lichti-Federovich, 1970), 1 mm bog thickness.
13	Western Saskatchewan (David, 1970), 3 cm in alluvial deposit. No original thickness estimate made. Suggests the presence of Mazama ash still farther east.
14-18	Approximate location of new discoveries of Mazama ash (R. E. Wilcox, personal communication, November 13, 1970).

(Continued on next page)

Table 2. (Continued)

Location	Description
19	Antelope Unit (Harward and Youngberg, 1969), 223 cm upland.
20	Huckleberry Springs (Harward and Youngberg, 1969), 224 cm upland.

contain Mazama ash, but have also provided thickness distributions along the major northeasterly lobe of ash deposition. It appears that the three data points used by Williams and Goles (1968) were not sufficient to describe the distribution of Mazama ash throughout the Pacific Northwest.

In order to estimate the volume of Mazama ash which fell beyond 100 km of Crater Lake, selected data on distribution and thickness of Mazama ash have been plotted as in Figure 5 (see also Table 2). The most reliable thicknesses of original ash fall are those obtained from bog sites. In a bog, reworking has been kept to a minimum and over-thickening can often be detected. In order to avoid error of over-estimation, care was taken to omit any measurement of layers which may have been mixed. Thicknesses taken from uplands of low relief have been used where bog data are absent. Reworking of the upland ash deposits is very common and estimates of original thickness are less reliable. A large amount of data for upland sites was examined but not used in these calculations in order to avoid overestimation. Nevertheless, it was clear that deposits of significant thickness are present along the northeastern axis at considerable distance from the source. Where upland thicknesses are uniform over large areas and correlate with nearby bog thicknesses, they are considered reliable. Mazama ash is also found in a variety of alluvial deposits. However, no thickness measurements from such environments have been used to

estimate original ash fall. Where quantitative data on original ash fall thickness are absent over large areas, it is generally due to bog-poor terrain or erosional environment and topography.

Two procedures have been employed in the evaluation of the volume of Mazama ash deposited throughout the Pacific Northwest. The first method uses analytical integration to approximate the volume contained in arcuate segments of the ash sheet (Figure 7). The second method entails graphical integration of an isopach map showing a thickness distribution suggested by available and most reliable data (Figure 5).

A plot of thickness of Mazama ash versus distance from the source (Figure 6) indicates that the radial distribution is described by a function of the form $Y = ae^{-br}$. Y is the thickness of Mazama ash, r is the distance from the source, and a and b are constants evaluated from Figure 6. The differential area swept out by angle θ of an arcuate segment is

$$dA = (\theta/360)(2 \pi r dr)$$

The volume of ash in the arcuate segment can be calculated by the relation

$$V = \int Y(r) dA$$

$$V = (\theta/360)(2 \pi a) \int_{r_1}^{r_2} r e^{-br} dr$$

$$V = (\theta/360)(2 \pi a)(e^{-br}) \left[-\frac{r}{b} - \frac{1}{b^2} \right]_{r_1}^{r_2}$$

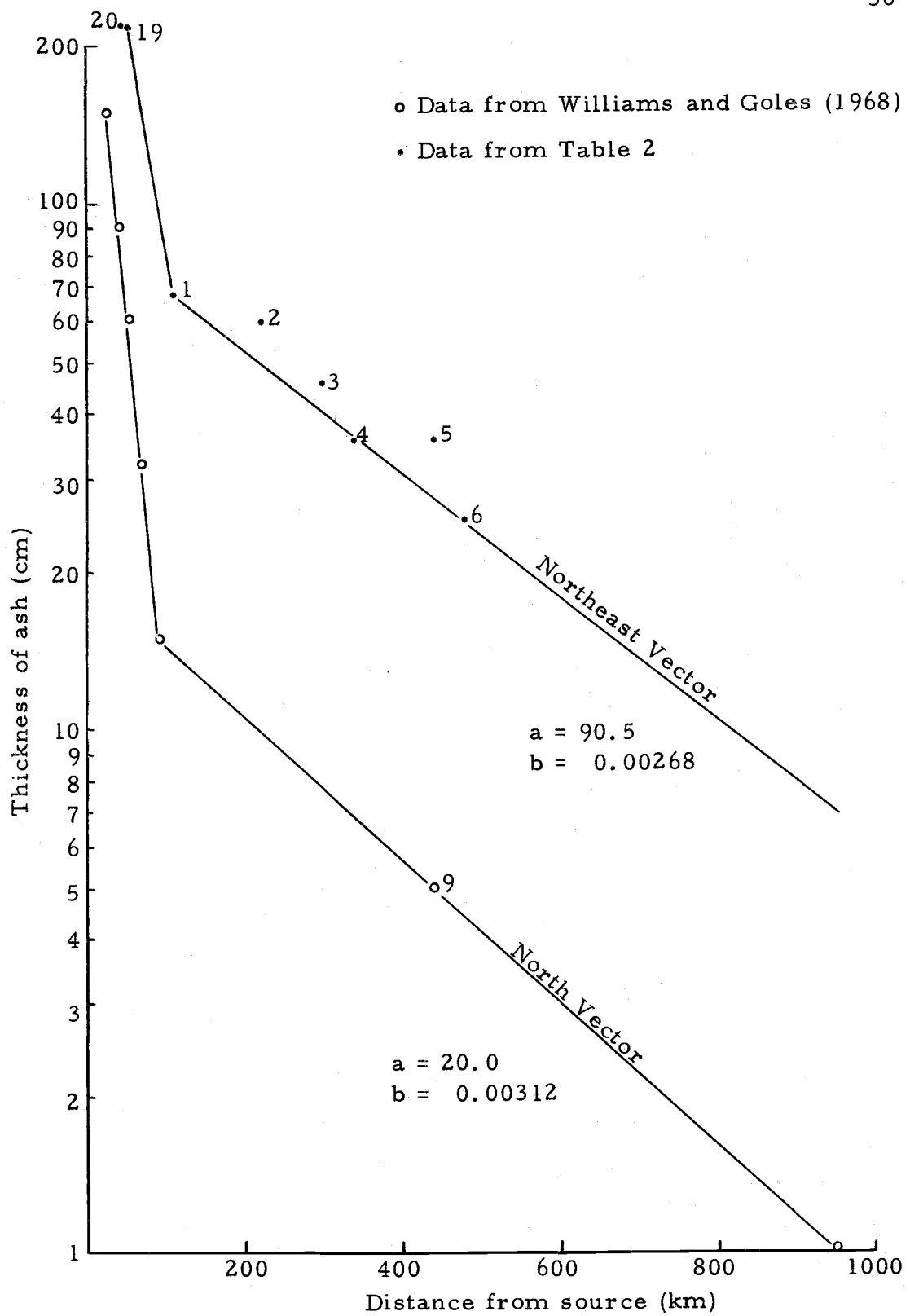


Figure 6. Mazama air-fall ash thickness along a north and northeast vector.

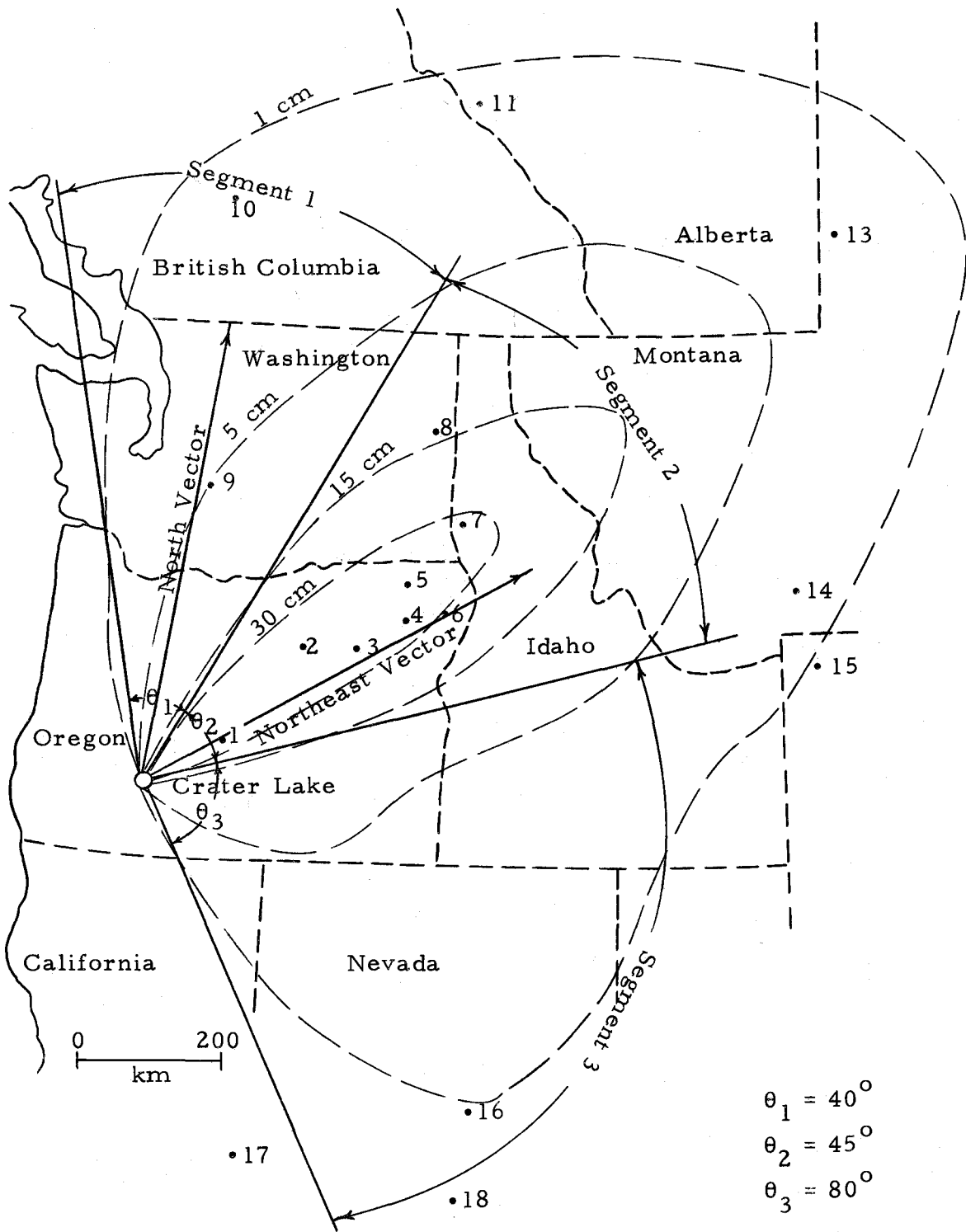


Figure 7. Directional parameters used in analytical estimation of ash volume.

The thickness of Mazama ash is a function of both distance and direction from the source. In order to account for variation of thickness with direction, the area containing Mazama ash has been divided into three segments (Figure 7). The thickness distribution along a north vector (Figure 6) adopted by Williams and Goles (1968) was used as an average distribution for segments 1 and 3. Limits of integration were set from 100 to 1500 km, and a combined volume of 40 km^3 was calculated. A northeast vector through Hurricane Creek (Figure 6) was considered an average distribution, and was used to calculate the volume of ash contained in segment 2 which is the major lobe of ash deposition. Limits of integration were set from 100 to 2000 km and a volume of 85 km^3 was calculated. The mathematical model based upon these considerations leads to the conclusion that 125 km^3 of Mazama ash fell beyond 100 km of Crater Lake. Although more data are needed to completely describe the distribution of Mazama ash, this analytical method provides a controlled estimate of the volume of ash beyond data points.

Graphical integration of the isopach representation (Figure 5) indicates that at least 100 km^3 of Mazama ash were deposited within the 1 cm isopach. Analytical integration suggests that 15-20 percent of this volume fell beyond the 1 cm isopach. It is therefore concluded that 100 km^3 is a minimum volume estimate for the total Mazama air-fall deposited beyond 100 km of Crater Lake.

Once the volume of ash is calculated, it must be corrected to magmatic volume. Mazama ash in bog sites has a bulk density of approximately 1.4 g/cc (Rai, 1971). Upland Mazama ash has a bulk density between 0.6 and 0.8 g/cc (Knox, Harris, Theisen and Borchardt)². All measured thicknesses used in this investigation have been corrected to a standard bulk density of 0.7 g/cc corresponding to average upland values. The bulk density of the magma with its gas in solution is assumed to have been approximately 2.4 g/cc. Therefore, the volume of ash calculated must be divided by a factor of 3.4 to obtain approximate magmatic volume.

If, as concluded above, at least 100 km³ and perhaps 125 km³ of Mazama ash were deposited beyond 100 km of Crater Lake, the magmatic volume represented by this ash would be 30-37 km³. Combining these new estimates with Williams' (1942) estimate of erupted material within the 100 km limit, the total volume erupted from Mount Mazama during the climactic eruption is between 57 and 64 km³. This total volume is in close agreement with Williams and Goles' (1968) estimate of the volume of Mount Mazama which disappeared due to engulfment. Therefore, it is concluded that there is no reason to suggest subterranean withdrawal of a portion of the magma. I attribute summit collapse to rapid removal of magma by

² Unpublished data. Soils Department, Oregon State University, Corvallis.

eruption of dacite pumice and basic scoria.

Granitic Fragments Associated with
the Culminating Eruptions

Diller and Patton (1902) first described granitic ejecta at Crater Lake as "light-colored granophyric secretions." Diller (p. 40) described one "boulder-like bomb" approximately 50 cm in diameter:

It had a blackened shell which was cracked to a little depth, and the cracks stood open like those of a bursted apple. The outside was very hard and glistened as if melted and glazed. Within the rock was very porous and pumiceous.

No plutonic fragments have been described in the main cone andesite, but Williams (1942) found evidence for granitic fragments enclosed in the post-caldera Wizard Island lavas. Taylor (1967) was the first to note the abundance and wide distribution of accidental granitic ejecta associated with the culminating eruptions.

Description of the Granitic Ejecta

Most of the granitic ejecta associated with the culminating eruptions appear to have undergone variable fusion, although some may never have been entirely crystalline. They generally contain a pumiceous interior surrounded by a dark, glassy rind. Light-colored, rounded plagioclase phenocrysts are suspended in the glassy rind, and sometimes exhibit a granophyric intergrowth with the enclosing glass. Inflation of the interior after chilling of the rind produced

breadcrust-type cracks (Figure 8). The color of individual fragments varies from white to black generally becoming darker with increasing glass content. Large, extensively melted fragments are abundant in the final crystal-rich basic scoria flows, and range up to 1.5 meters in diameter. These fragments have a vitrophyric texture and are commonly dark brown to black in color. Presence of breadcrust cracks, inflation, resorbed plagioclase phenocrysts, and absence of hornblende can be used to distinguish the extensively melted fragments from surrounding crystal-rich scoria bombs. Some of the fragments appear as light-colored, granular aggregates which have been inflated but contain no glassy rind or cracks, and probably represent the interiors of fragments. A small percentage of the fragments are holocrystalline, and there are two distinct types recognizable in hand specimen. The first type is fine-grained, uniformly gray in color, and has been found up to 50 cm in diameter. These fragments resemble andesite and can only be identified upon close inspection. Their holocrystalline character and presence of miarolitic cavities containing biotite are distinctive. No melted equivalents of these fine-grained fragments have been recognized. The second type of holocrystalline fragment is coarse-grained (1-2 mm) and appears to represent the unmelted equivalent of the glassy fragments. The color of these coarse-grained fragments is white to light-gray, and biotite and quartz can easily be recognized with a hand lens. Biotite and quartz



Figure 8. Melted granitic fragment. Note the glassy rind with large cracks that reveal the pumiceous interior. This fragment was found approximately 1 km south of Dutton Cliff (scale is in inches).

have not been identified in other eruptive products associated with Mount Mazama. The size of ejecta generally increases with distance from the caldera rim with the largest fragments showing the greatest evidence of melting. Holocrystalline varieties greater than 15 cm in diameter have not been found. Fine-grained, dark inclusions are rather common in the coarse-grained fragments, but have not been observed in the fine-grained fragments. These inclusions are generally subrounded to angular, show no evidence of melting, and often stand out conspicuously in partially melted fragments.

In summary, the bulk of granitic ejecta exhibit evidence of melting. Probably the single most distinctive feature of the melted ejecta is their shiny, vitrophyric rind with breadcrust cracks. Most fragments are extremely clean showing no evidence of adhering basic scoria. Holocrystalline fragments are subordinate both in size and abundance, but their light-color, presence of biotite and quartz, and holocrystalline texture is distinctive.

Distribution of Granitic Ejecta

Scattered granitic fragments (both holocrystalline and hypocrystalline) are found associated with all of the explosive dacitic eruptions of Mount Mazama. Such fragments are especially conspicuous in the welded tuff sections of Cottage Rock and Wineglass. However, the major concentration of large granitic fragments is found

in deposits formed by the last dying phases of the culminating eruptions. Although scattered ejecta may be found in abundance virtually everywhere around the caldera rim, the distribution of extensive deposits containing large numbers of granitic fragments is more restricted and is presented in Figure 9.

Granitic fragments are of infrequent occurrence in the dacite pumice deposits of the culminating eruptions. They are also scarce in the initial basic scoria flows which abruptly followed the eruption of dacite. Melted granitic fragments first appeared in significant quantities near the end of the basic scoria eruption. These final scoria deposits are characterized by large quantities of lithic fragments and crystal-rich scoria bombs. Melted granitic fragments contained in these crystal-rich scoria flows range up to 1.5 meters in size and may be found 7-8 km from the caldera rim.

Violence of eruption decreased rapidly after appearance of the crystal-rich basic scoria. No longer did the erupted material rush down the volcano as glowing avalanches, but instead, fell on the upper slopes forming a chaotic deposit of crystal-rich scoria, andesitic fragments, and granitic fragments (both melted and holocrystalline). Bombs of mixed light and dark pumice are often scattered among the ejecta. These final chaotic deposits generally do not extend more than 2-3 km downslope from the caldera rim, but clearly overlie earlier basic scoria flows. They are characteristically reddish-brown in

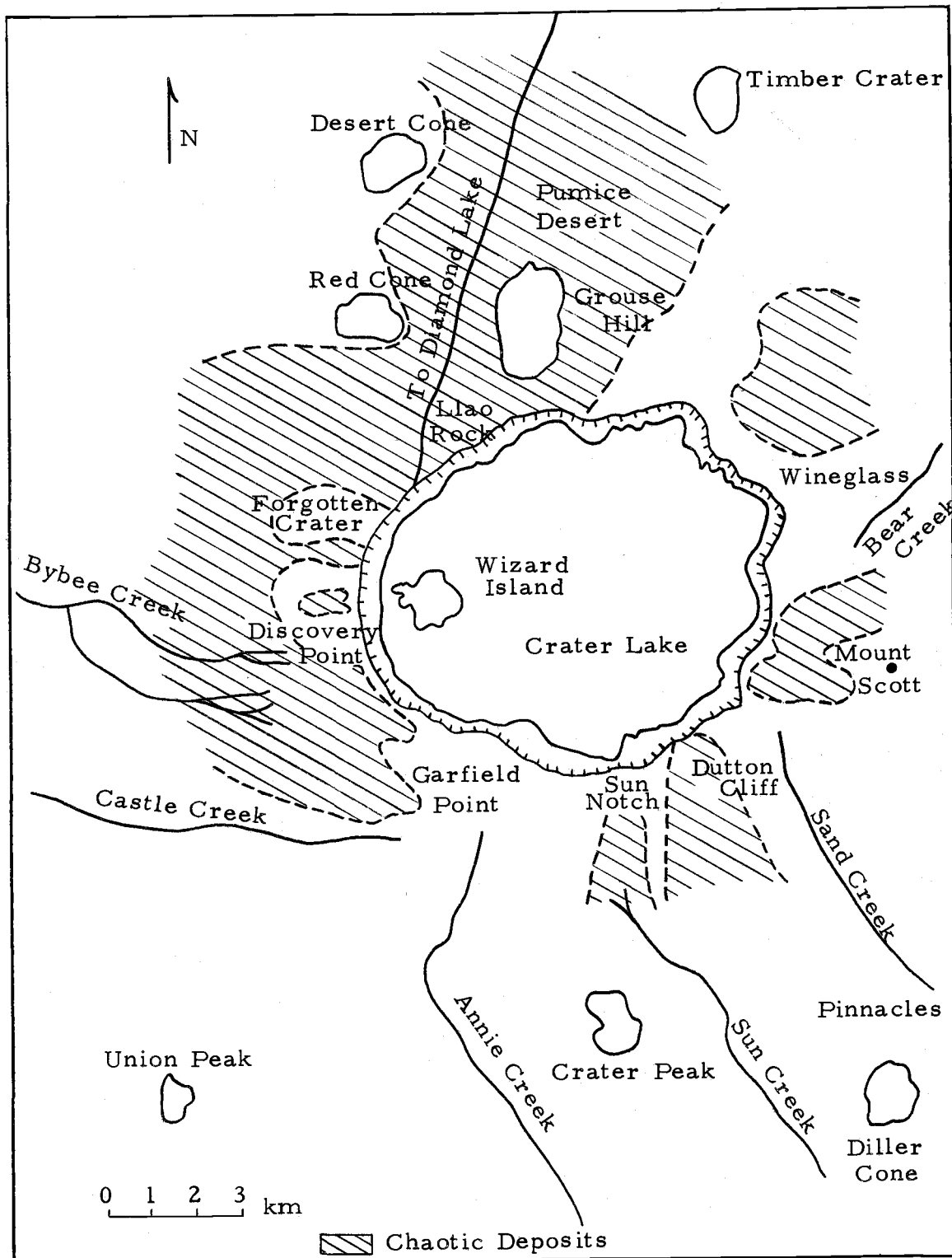


Figure 9. Distribution of granodiorite-bearing chaotic deposits of the final dying eruptions from Mount Mazama.

color which helps to distinguish them from underlying smoke-gray or brown basic scoria flows. Cross-sections of these non-stratified deposits (usually 5-10 meters thick) are often exposed at the caldera rim (Figure 10). The deposits overlie those of stratified coarse dacite pumice and basic scoria.

In summary, it appears that the largest and most intensely melted fragments were erupted first. As the energy of the eruptions decreased, the size and degree of melting of the granitic ejecta decreased. These final ejecta were deposited in chaotic layers on the upper slopes of the volcano and marked the final dying explosions of the culminating eruptions. Thus, during the final stages of eruption, decreasing violence is correlated with increasing content of crystals, andesite fragments, and granitic fragments in the magma.

Petrography of the Granitic Fragments

On the basis of petrographic investigation, two distinct groups of granitic fragments can be distinguished. The first group is fine-grained, usually containing less than five percent of grains greater than 1 mm in length, and exhibits no evidence of melting. The second group is decidedly coarser-grained, containing 20-40 percent of phenocrysts larger than 1 mm in size. This group of fragments exhibits a melting sequence, ranging from holocrystalline varieties to fragments containing 60-70 percent glass. Holocrystalline varieties



Figure 10. Cross-section of chaotic deposits containing andesite, granitic fragments, and crystal-rich basic scoria. Note stratified dacite pumice directly beneath the chaotic deposits.

appear to be petrographically similar to granodiorite from the Tatoosh Pluton located at Mount Rainier, Washington (Fiske et al., 1963). These authors suggest that the complexly zoned plagioclase phenocrysts and granophyric intergrowths in the groundmass indicate crystallization under subvolcanic conditions characterized by a highly variable physiochemical environment.

Holocrystalline, coarse-grained fragments contain between 20 and 40 percent subhedral, complexly zoned and intergrown plagioclase phenocrysts ranging in length from 1-3 mm. These phenocrysts are zoned from labradorite at the center to sodic andesine near the margins. Biotite and hornblende are present as phenocrysts generally comprising three to five percent of the rock. These minerals seldom exceed 1.5 mm in length and are characteristically associated with small blebs of magnetite. Biotite is green to greenish-brown and is generally present as flakes exhibiting ragged and embayed edges (Figure 11). Hornblende is greenish-brown and occurs either as longish granular or euhedral prismatic crystals. The groundmass (grains below 0.5 mm in diameter) is composed of plagioclase feldspar (sodic andesine-oligoclase), quartz, orthoclase, biotite, and hornblende. Plagioclase is generally subhedral while quartz and orthoclase are present as anhedral grains with orthoclase often mantling plagioclase phenocrysts. Granophyric intergrowths comprise from 15-25 percent of the groundmass (Figure 12), and are



Figure 11. Photomicrograph of unmelted coarse-grained granitic fragment. - Note phenocryst of biotite with ragged and embayed edges but showing no evidence of replacement. Granophyric texture is minor.



Figure 12. Photomicrograph of coarse-grained granitic fragment exhibiting little or no glass. Note development of granophyric intergrowths in the orthoclase which characteristically mantles plagioclase phenocrysts.

present as both intergrowths of quartz with orthoclase, and intergrowths of quartz in groundmass plagioclase. Granophyric intergrowths are particularly conspicuous in the orthoclase which mantles plagioclase. Either the outer edge of the mantle is intergrown with quartz or the intergrowths begin near the plagioclase edge with little or no free mantle growth visible. Accessory minerals of apatite and zircon are particularly conspicuous and are often found included in the plagioclase phenocrysts.

As the granitic fragments were subjected to higher temperatures distinct mineralogical changes occurred. Modal analyses of a representative sequence of coarse-grained fragments are presented in Table 3 and mineralogical changes versus degree of melting are plotted in Figure 17. The first glass appears in contact with the granophyric intergrowths producing a lobed fringe which is interwoven or intergrown in such a fashion that it resembles the granophyric intergrowths themselves (Figure 13). Apparently, quartz and potassium feldspar produce a eutectic melt at points of contact. With appearance of glass, hornblende and biotite exhibit discoloration and sometimes partial replacement by granular pyroxene can be noted. When five percent or more glass is present, pyroxene completely replaces hornblende and biotite (Figure 14). The pyroxene is both hypersthene and augite occurring in clusters of loosely aggregated prismatic grains. These aggregates often contain hundreds of small



Figure 13. Photomicrograph of slightly melted coarse-grained granitic fragment. Note development of glass in the granophyric intergrowths.



Figure 14. Photomicrograph of melted coarse-grained granitic fragment. Note the granular aggregates of pyroxene replacing a large flake of biotite.

prismatic grains and are constantly associated with magnetite.

The overall abundance of granophyric intergrowth appears to increase until approximately ten percent glass is present. At this point, almost all the orthoclase and groundmass plagioclase contains some form of intergrowth. The invading glass destroys the granophyric intergrowths associated with potassium feldspar first, and breaks up the feldspar into rectangular or polygonal forms with more or less parallel arrangement, until only a skeleton remains. As glass content increases, granophyric intergrowths are destroyed until most of the groundmass has been replaced by glass. The last minerals to survive this process of remelting are rounded quartz grains, partially resorbed pyroxene aggregates, and resorbed phenocrysts of plagioclase exhibiting spongy, lobate fringes (Figure 15).

Fine-grained granitic fragments are uniform petrographically (Figure 16). A modal analysis of fragment 69-5 is presented in Table 3. These fragments generally contain from two to seven percent plagioclase phenocrysts ranging in length from 0.5-1.0 mm. The plagioclase is broken and complexly zoned from labradorite to sodic andesine. The groundmass (less than 0.5 mm) consists of biotite, hornblende, quartz, plagioclase, and orthoclase. Accessory minerals are magnetite, augite, and zircon. The content of biotite and hornblende varies from three to five percent with biotite generally predominating. Individual crystals are small (less than 0.5 mm in

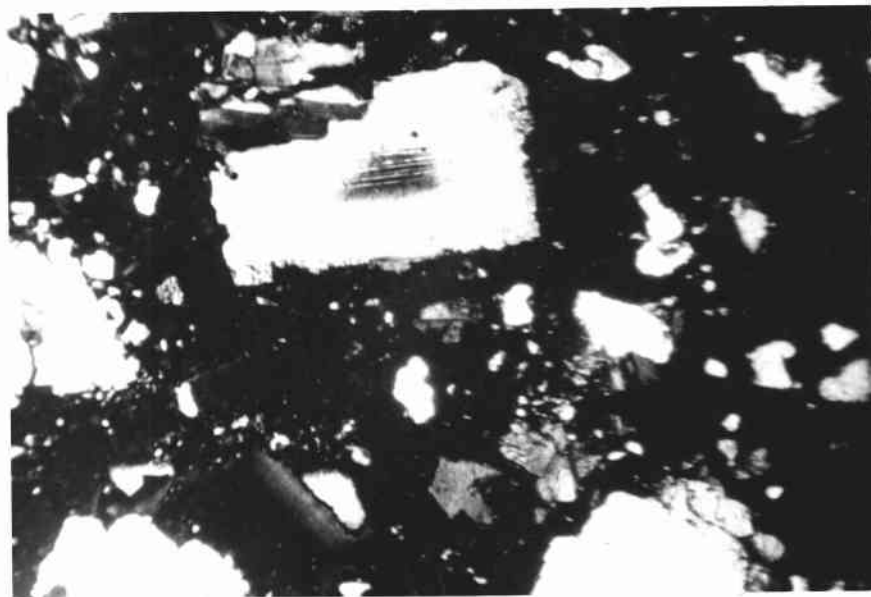


Figure 15. Photomicrograph of intensely melted granitic fragment. Note the spongy melting around the edges of the remaining plagioclase phenocrysts. A few scattered pyroxene aggregates and rounded quartz grains are present.

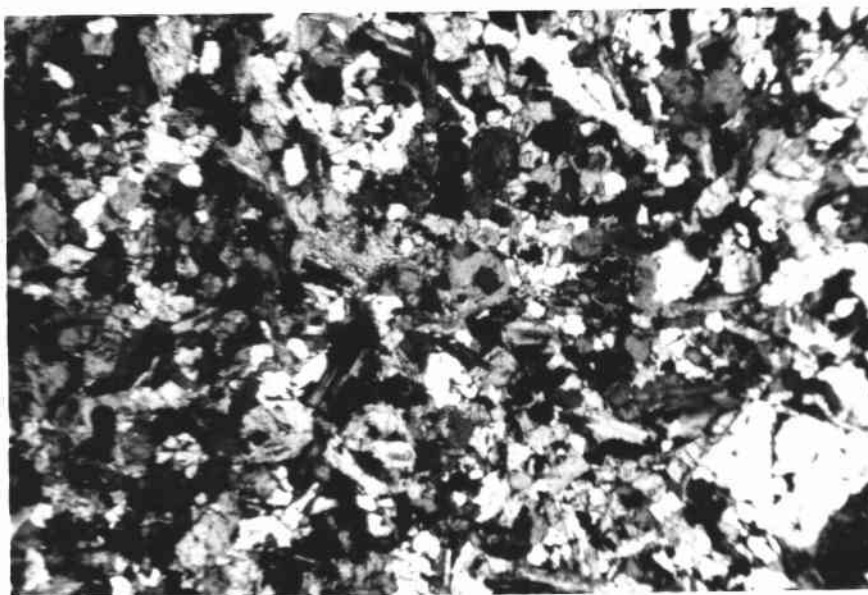


Figure 16. Photomicrograph of fine-grained granitic fragment. Plagioclase phenocrysts are minor, but quartz is abundant as small grains in the groundmass. Granophyric texture is present but not conspicuous.

Table 3. Modal analyses of granitic ejecta associated with the culminating eruptions. (Fragments 69-4 through CL-75 are coarse-grained and exhibit a typical melting sequence. Fragment 69-5 is a representative fine-grained fragment.)

	<u>69-4</u>	<u>CL-28</u>	<u>CL-80</u>	<u>69-9</u>	<u>CL-70</u>	<u>CL-107</u>
Glass	none	none	none	trace	2.0	6.0
Plag	50.0	49.0	52.0	46.0	50.0	47.0
Qtz	16.5	14.0	10.0	13.5	1.0	2.5
K-spar	12.0	12.0	6.0	8.5	1.0	3.5
Granophyric intergrowth	12.5	18.0	23.0	24.5	40.0	34.0
Hb. and biotite	9.0	7.0	9.0	7.5	1.0	none
Secondary pyroxene	none	none	none	none	5.0	7.0
	<u>69-11</u>	<u>CL-30</u>	<u>CL-71</u>	<u>CL-113</u>	<u>69-10</u>	<u>69-8</u>
Glass	8.0	14.0	18.5	20.0	24.0	27.0
Plag	43.0	40.0	53.0	51.0	45.0	48.0
Qtz	6.0	3.0	5.0	8.0	6.5	9.0
K-spar	6.0	6.0	4.5	7.0	5.5	5.0
Granophyric intergrowth	33.0	29.0	13.0	9.0	13.0	6.0
Hb. and biotite	none	none	none	none	none	none
Secondary pyroxene	4.0	8.0	6.0	5.0	7.0	5.0
	<u>69-7</u>	<u>CL-108</u>	<u>CL-111</u>	<u>69-14</u>	<u>CL-75</u>	<u>69-5</u>
Glass	28.0	34.5	54.0	58.0	65.0	none
Plag	50.0	49.0	41.0	34.5	31.0	55.0
Qtz	5.0	9.0	3.0	3.5	2.5	19.0
K-spar	2.0	2.5	none	trace	none	18.0
Granophyric intergrowth	11.0	none	none	none	none	5.0
Hb. and biotite	none	none	none	none	none	3.0
Secondary pyroxene	4.0	5.0	2.0	4.0	1.5	none

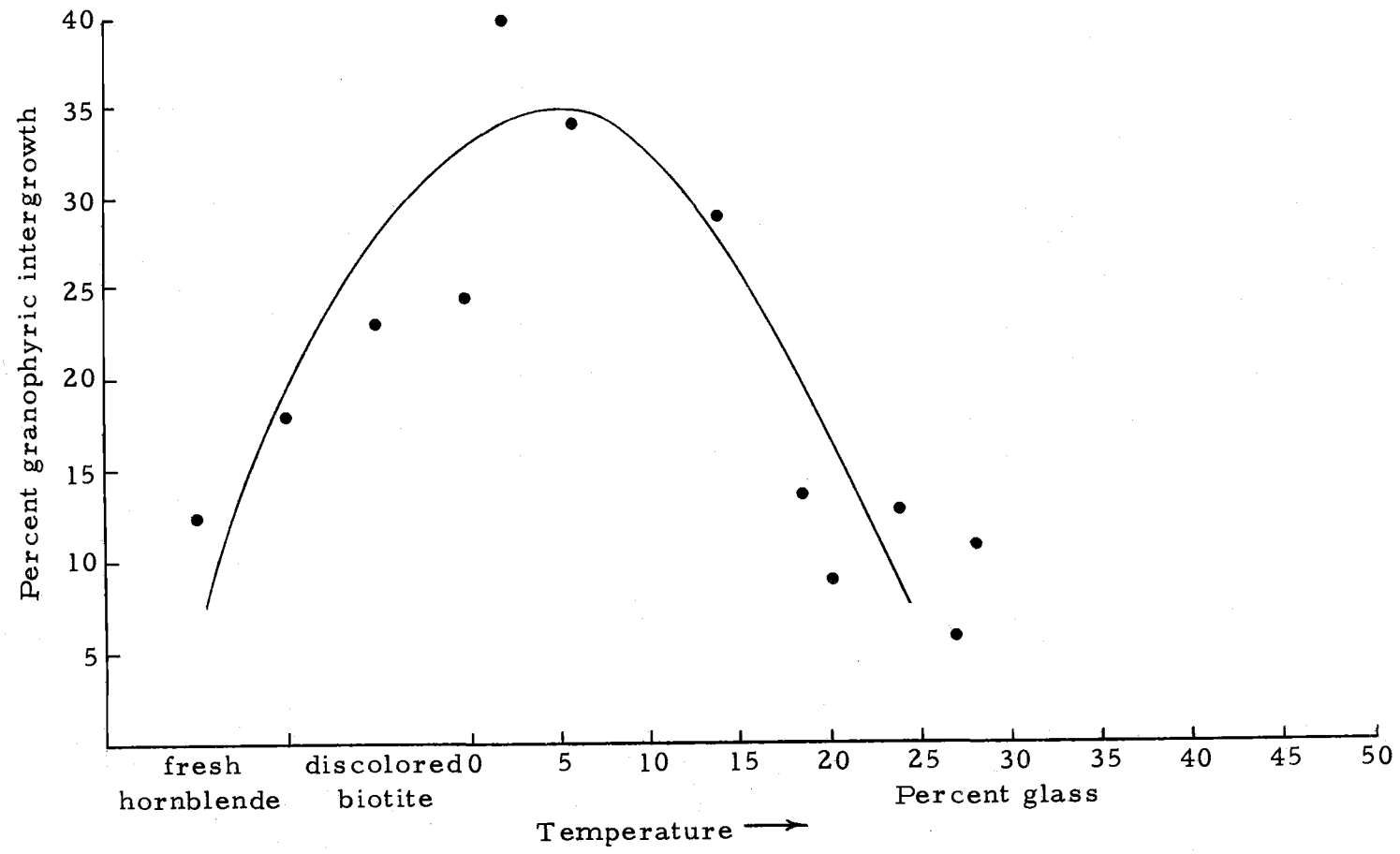


Figure 17. Percent granophyric texture versus increased temperature as inferred from alteration of mafic silicates and content of glass.

diameter), subhedral, commonly show discoloration (from greenish-brown to reddish brown), and are characteristically associated with magnetite. No evidence of replacement of biotite and hornblende by pyroxene has been noted. Groundmass plagioclase, orthoclase, and quartz are intimately intergrown. Plagioclase occurs as subhedral to euhedral laths, and quartz and orthoclase form anhedral. Granophyric intergrowths are present in the groundmass, but they generally comprise less than ten percent of the rock. No evidence of glass has been noted in these fine-grained fragments.

In general, the fine-grained fragments contain fewer phenocrysts of plagioclase, biotite, and hornblende, and contain more groundmass quartz and orthoclase than the coarse-grained fragments. No glass has been observed. The coarse-grained fragments contain conspicuous granophyric intergrowths and exhibit a complete sequence of melting. Fine-grained inclusions are abundant in the coarse-grained fragments, but have not been observed in the fine-grained fragments. These inclusions are composed of fine-grained (less than 0.5 mm in diameter) aggregates of plagioclase laths, augite grains, and magnetite with some interstitial quartz and orthoclase. Small blebs of glass are sometimes present in the interstitial quartz and orthoclase.

Chemistry of the Granitic Fragments

Figure 18 is a Harker diagram presenting new analyses in which

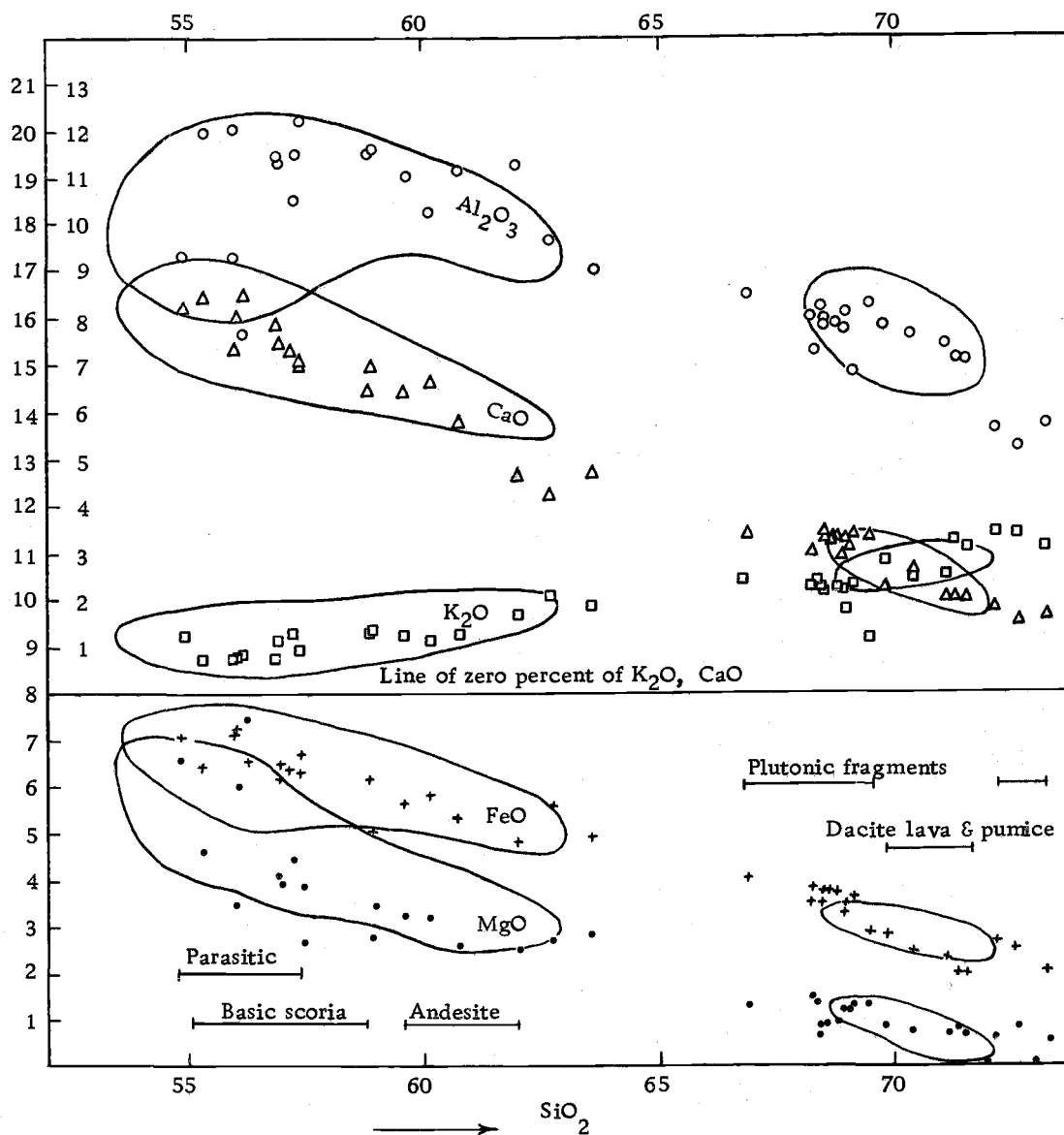


Figure 18. Harker variation diagram of Crater Lake rocks. Analyses obtained by X-ray fluorescence. Enclosures taken from Figure 4.

ignited sample powders were fused in anhydrous lithium tetraborate flux, and cast into buttons. A polished face of each sample button was analysed for Si, Al, Fe, Ca, Mg, K, and Ti using a Cr-target X-ray source with appropriate analysing crystals and detection systems. Analytical accuracy and precision were checked by replicate analyses of U. S. G. S. rock standards BCR-1, AGV-1, GSP-1 and G-2. All values were accurate to within one percent of the amount present.

Enclosures in Figure 18 are taken from Figure 4 and it is evident that the new fluorescent analyses are consistent with published analyses of previous authors. Chemical variations of granitic ejecta, in particular, are consistent with variation of the dacite eruptive products of Mount Mazama. Coarse-grained fragments are slightly more mafic than dacite pumice from the culminating eruptions and earlier dacite lavas. Fine-grained granitic fragments are slightly more silicic than dacite lava and pumice. Deviations from the major trend of Mazama rocks are restricted to crystal-rich scoria bombs and extensively melted granitic fragments.

According to Turner and Verhoogen (1960), granodiorite is chemically equivalent to dacite. Williams, Turner and Gilbert (1954) define granodiorite as a rock intermediate between quartz monzonite and quartz diorite with alkali feldspar comprising between one-eighth and one-third of the total feldspar. Therefore, the granitic ejecta at Crater Lake can be classified as biotite- and hornblende-bearing

1. Lava flow near crater of Red Cone.
2. Basic scoria bomb collected near the head of Sand Creek.
3. Crystal-rich basic scoria bomb found near caldera rim.
4. Lava flow from north flank of Bald Crater.
5. Hornblende-rich basic scoria bomb from the Pumice Desert.
6. Highly indurated basic scoria exposed along Sand Creek.

7. Highly indurated basic scoria exposed in Castle Creek.
8. Lava from north slope of Crater Peak.
9. Basic scoria bomb from Pumice Desert.
10. Well indurated basic scoria from Duwee Falls.
11. Hornblende-rich basic scoria bomb from Pumice Desert.
12. Loosely indurated basic scoria from Annie Creek.

13. Lava flow from Hillman Peak.
14. Lava from Wizard Island.
15. Lava from Merriam Cone (submerged under Crater Lake). Received courtesy of Crater Lake National Park Service.
16. Lava from Sentinel Rock.
17. Fine-grained inclusion found in granitic ejecta of the culminating eruptions.
18. Fine-grained inclusion found in granitic ejecta of the culminating eruptions.

Table 4. Chemical analyses of the eruptive products associated with Mount Mazama. ^a

	<u>1</u>	<u>2</u>	<u>3</u>	<u>4</u>	<u>5</u>	<u>6</u>
SiO ₂	54.87	55.35	56.0	56.03	56.22	56.90
Al ₂ O ₃	17.38	20.05	20.56	17.34	15.66	19.58
FeO	7.0	6.40	7.11	7.20	6.52	6.17
CaO	8.20	8.40	7.31	8.0	8.53	7.83
MgO	6.60	4.60	3.46	6.00	7.52	4.11
K ₂ O	1.20	0.70	0.79	0.80	0.90	0.78
TiO ₂	1.00	0.77	1.13	1.00	0.90	0.87
	<u>7</u>	<u>8</u>	<u>9</u>	<u>10</u>	<u>11</u>	<u>12</u>
SiO ₂	56.98	57.22	57.40	57.40	58.85	58.90
Al ₂ O ₃	19.36	18.54	20.30	19.57	19.50	19.60
FeO	6.45	6.31	6.65	6.28	6.15	5.00
CaO	7.45	7.30	7.17	7.09	6.43	7.0
MgO	3.92	4.53	2.66	3.95	2.80	3.50
K ₂ O	1.10	1.28	0.97	0.91	1.20	1.30
TiO ₂	0.85	0.95	1.07	0.91	1.05	0.80
	<u>13</u>	<u>14</u>	<u>15</u>	<u>16</u>	<u>17</u>	<u>18</u>
SiO ₂	59.63	60.14	60.75	62.00	62.69	63.58
Al ₂ O ₃	19.00	18.25	19.20	19.35	17.71	17.07
FeO	5.66	5.80	5.38	4.83	5.60	4.92
CaO	6.46	6.63	5.87	4.63	4.20	4.72
MgO	3.23	3.21	2.64	2.51	2.70	2.80
K ₂ O	1.21	1.10	1.27	1.73	2.10	1.80
TiO ₂	0.73	0.73	0.75	0.72	0.68	0.65

(Continued on next page)

19-24. Coarse-grained granodiorite fragments.

25-30. Coarse-grained granodiorite fragments.

31. Dacite lava from Cleetwood Flow.

32. Dacite lava from Llao Rock.

33. Hypersthene-hornblende dacite from
submerged dome east of Wizard Island.

Received courtesy of Crater Lake National
Park Service.

34. Lava from Redcloud Cliff.

35. Fine-grained granodiorite fragment.

36. Coarse air-fall dacite pumice of the
culminating eruptions.

37. Fine-grained granodiorite fragment.

Table 4. (Continued)

	<u>19</u>	<u>20</u>	<u>21</u>	<u>22</u>	<u>23</u>	<u>24</u>	
SiO ₂	66.90	68.25	68.35	68.45	68.45	68.50	
Al ₂ O ₃	16.47	16.08	15.30	16.02	16.25	15.82	
FeO	4.00	3.56	3.94	3.59	3.89	3.82	
CaO	3.40	3.00	3.32	3.38	3.17	3.26	
MgO	1.30	1.52	1.30	0.92	0.61	0.97	
K ₂ O	2.40	2.21	2.38	2.25	2.25	2.14	
TiO ₂	0.65	0.50	0.57	0.56	0.58	0.58	
	<u>25</u>	<u>26</u>	<u>27</u>	<u>28</u>	<u>29</u>	<u>30</u>	
SiO ₂	68.8	68.94	69.00	69.10	69.45	69.80	
Al ₂ O ₃	15.89	15.70	16.18	14.82	16.25	15.89	
FeO	3.67	3.22	3.42	3.61	2.91	2.85	
CaO	2.96	3.22	3.11	3.30	3.32	2.24	
MgO	0.97	1.20	1.24	1.30	1.35	0.82	
K ₂ O	2.25	2.21	1.76	2.31	1.14	2.85	
TiO ₂	0.51	0.50	0.52	0.55	0.60	0.51	
	<u>31</u>	<u>32</u>	<u>33</u>	<u>34</u>	<u>35</u>	<u>36</u>	<u>37</u>
SiO ₂	70.40	71.14	71.35	71.55	72.15	72.65	73.24
Al ₂ O ₃	15.73	15.63	15.25	15.14	13.62	13.22	13.74
FeO	2.42	2.36	2.00	2.00	2.70	2.58	2.02
CaO	2.62	2.00	2.00	2.00	1.80	1.49	1.61
MgO	0.70	0.70	0.80	0.70	0.70	0.89	0.60
K ₂ O	2.47	2.52	3.25	3.00	3.40	3.37	3.08
TiO ₂	0.47	0.45	0.37	0.45	0.38	0.35	0.35

^aAll analyses performed by X-ray fluorescence.

granodiorite.

Origin and Significance of the Granitic Ejecta

The dacite magma which fed the culminating eruptions appears to have been emplaced approximately 12,000 years ago. If this is true, the dacite magma cooled for approximately 5000 years before it was violently expelled. Since there is no evidence of eruption during this period, the magma apparently had reached a condition approaching equilibrium.

The purpose of this section is to evaluate the cooling history of such a magma. Many models can be developed for this evaluation depending upon the shape and depth of the magma chamber. It is certainly not the intent of this author to solve the many complex combinations that might arise. Instead, one model (applicable to the situation at Crater Lake) will be evaluated to obtain an estimate of the extent of crystallization that could occur in a dacite magma of 70 km³ volume lying at a depth of 5 to 10 km, during this period of quiescence.

A spherical magma reservoir would be the most stable toward cooling. According to Shimazu (1960), when thermal and mechanical stabilities are both taken into consideration, the shape of a magma reservoir is a disc-like sheet (ratio of horizontal extension to thickness 6:1). Since the dacite magma which fed the culminating eruptions

appears to have been stable, a disc-like configuration will be used in the thermal analysis. Assuming that the volume of injected dacite magma was approximately 70 km^3 , this configuration would result in a magma reservoir approximately 56 km^2 by 1.25 km thick. Thus, the area of a vertical projection of the magma chamber would be almost identical to the present area of the caldera floor.

The author agrees with Williams (1942) that the magma which fed the culminating eruptions was emplaced at shallow depth beneath Mount Mazama. Otherwise, collapse would not have been confined to the summit and resultant caldera formation would not have been possible. The depth of the magma chamber is estimated to be 5-10 km.

Jaeger (1957) has solved the problem of a cooling intrusive sheet set up by Larsen (1945), and considered to be typical of a shallow granitic intrusion. The intrusion was assumed to have been emplaced rapidly with respect to the time of solidification. The form of the intrusion was assumed to have been a flat sheet of thickness D in a vertical direction and extending indefinitely in the perpendicular directions. The magma was assumed to have been intruded at its liquidus temperature, and cooling was by conduction only.

Jaeger's solution (Figure 19) indicates that solidification is complete after $0.016 D^2$ years (D = thickness in meters of intrusive sheet). At Crater Lake with $D = 1.25 \text{ km}$, solidification would be

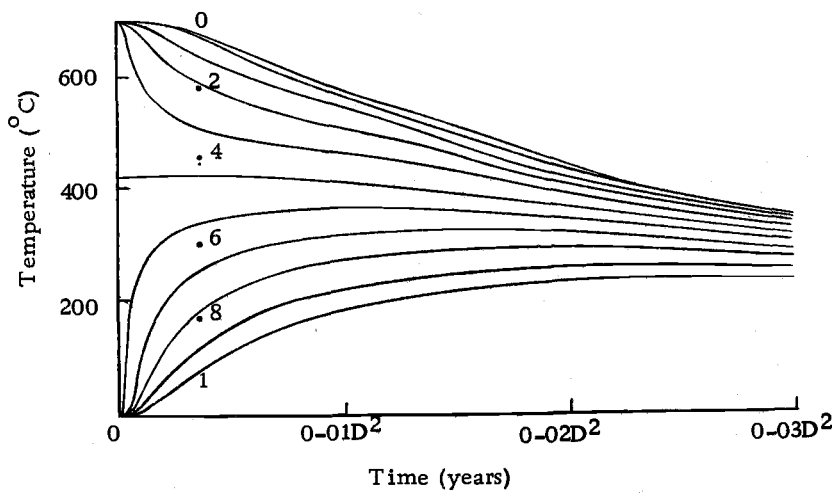


Figure 19. Temperature T at various points in an intrusive sheet of thickness D (meters) for which initial temperature $T_2 = 700^\circ\text{C}$, temperature of complete crystallization $T_1 = 500^\circ\text{C}$, and latent heat $L = 80 \text{ cal/gm}$. The numbers on the curves are distances from the center measured in fractions of the total thickness. (After Jaeger, 1957)

complete in 25,000 years. Jaeger (1957) also gives a relationship for distance X (meters) from the contact in which crystallization would occur during time t:

$$X = 9.5 \lambda (t)^{1/2}$$

Using Jaeger's calculated value of $\lambda = 0.137$ and a Mazama cooling interval $t = 5000$ years, $X = 90$ meters. For the model presented, this crystallized margin would correspond to approximately 15 percent of the injected magma. Williams and Goles (1968) estimate that the dacite magma contained between 8 and 15 km³ of crystals at the time of eruption. Assuming the volume of erupted dacite magma approached 60 km³, it is concluded that the dacite magma contained between 13 and 25 percent crystals at the time of eruption. Therefore, Jaeger's solution of this model is consistent with the degree of crystallization observed at Crater Lake, and demonstrates that a dacite magma could exist at shallow depth for 5000 years and develop a crystallized rind of sufficient thickness to supply abundant fragments of granodiorite.

Jaeger's solution does not account for emplacement of magma in a relatively high temperature subvolcanic environment that may have existed beneath Mount Mazama. Therefore, this solution may give a minimum time of solidification for the dacite magma at Crater Lake. If a more realistic model demands a longer period of cooling, a revision of the estimated time of emplacement may be necessary.

Thermal considerations indicate that a crystallized granodiorite

margin could have developed around the dacite magma which fed the culminating eruptions. The chemistry and mineralogy of the granodiorite fragments associated with the final phases of eruption are certainly consistent with such an origin. Therefore, it is concluded that the granitic ejecta of the culminating eruptions do not represent unrelated basement rocks, but instead, are merely the solidified margin of the dacite magma which crystallized between the time of high-level emplacement and culminating eruption (approximately 5000 years).

The partially melted granodiorite fragments generally have a glassy rind which was fractured by vesiculation of the gas-rich interiors. This glassy rind probably formed by chilling of the fragments upon ejection. The inflated, pumiceous interiors and fractured glassy rinds indicate that exsolution of gas occurred after chilling while the fragments were still partially liquid. Vesiculation of the fragments after ejection indicates that they were melted in a high pressure environment and then transported rapidly to the surface before they could lose their gas content.

It appears that the magma which produced the basic scoria occupied the bottom portion of the dacite magma chamber, and rested upon a floor of granodiorite. Assimilation of the granodiorite by the high-temperature basic scoria magma was pronounced wherever they were in contact. The fine-grained, silicic fragments were unmelted

because they occupied the upper portions of the crystallized margin. Coarse-grained granodiorite fragments crystallized around the lower margin of the chamber and were extensively melted along their contact with basic scoria magma. Extent of melting of the granodiorite decreased away from the contact zone, and eruption of large quantities of this crystallized rind produced a complete sequence of melted, partially melted, and fresh granodiorite fragments.

The zone of granodiorite assimilation was probably not very thick, as temperature would decrease rapidly away from the contact (Jaeger, 1957). Destruction of hydrous phases in the granodiorite would release water in a form which could become disseminated through a contact zone of basic scoria magma. Abnormally high water vapor pressure and decreased temperature along this contact zone would promote the stability of hornblende in the mafic magma. Hamilton and Anderson (1968) show from experimental studies that hornblende may become the stable phase in mafic magmas at high water vapor pressure. High water vapor pressure may have also developed along the contact between the dacite and basic scoria magmas. However, transfer of water to the underlying basic scoria magma would have to occur by molecular diffusion which is much too slow to significantly alter equilibrium conditions during the time available (Matsuo, 1961).

The basic scoria deposits are heterogeneous, containing bombs

of crystal-aggregates (Noble et al., 1969) enclosed in a comminuted matrix of glass and crystals of pyroxene, plagioclase, olivine, and hornblende. Hornblende is particularly conspicuous in the later scoria flows; in the Pumice Desert, bombs composed almost exclusively of hornblende prisms and glass can be found. Fresh olivine nuclei in hornblende phenocrysts from basic scoria have been described (Diller and Patton, 1902; Williams, 1942; McBirney, 1968). Phenocrysts of fresh olivine up to 1 mm in diameter constitute up to five percent of some basic scoria bombs. The close association with fresh olivine suggests that this hornblende did not crystallize from a magma as siliceous as the dacite, but probably formed in a basaltic andesite (basic scoria) magma. It was, therefore, the assimilation of granodiorite along a narrow contact zone at the base of a magma chamber which accounts for the concentration and heterogeneous distribution of hornblende and partially melted granodiorite fragments in the late-stage eruptive deposits. Banded pumice bombs associated with these final eruptions probably represent mixing of the melted granodiorite and basic scoria along the contact zone.

It appears that the last dying explosions actually ripped up portions of the floor and sides of the chamber, and deposited this material as a chaotic layer on the upper slopes of the volcano. Rock bursts from the margins of the chamber probably provided the unmelted granodiorite fragments of the last dying eruptions. These

unmelted fragments either represent granodiorite from the upper margins of the chamber, or granodiorite which was too far removed from contact with basic scoria magma to be melted. The partial-melt sequence of granitic ejecta among the final deposits of the culminating eruptions strongly indicates that the basal margins of the magma chamber had been reached by the eruptive process, and that the entire magma chamber (approximately 60 km^3) had been evacuated.

ORIGIN OF CRATER LAKE CALDERA: A NEW MODEL

Crater Lake is one of many Krakatoan type calderas scattered along the Circum-Pacific andesite belt. However, the number of calderas is small compared to the large number of andesite volcanoes which are not associated with calderas. For example, the Cascade Range of California, Oregon, and Washington contains many large, young andesitic volcanoes, but Mount Mazama is the only one which contains a recent caldera.

Krakatoan type calderas are formed by the collapse of the summit of pre-existing composite volcanoes following copious eruptions of magma as pumice-falls and pumice-flows (Williams and McBirney, 1968). These culminating eruptions issue from summit vents or from fissures on the flanks of the cone. Activity begins with eruption of pumice and proceeds toward eruption of fluidized ash-flows. These ash-flows (usually dacite or rhyolite) generally become more mafic and crystal-rich during the final phases of eruption. Many Krakatoan type calderas have been formed by eruption of a silicic magma followed closely by a more mafic magma. Heterogeneous eruption of mafic and silicic pumice or basic scoria toward the end of eruptions at Crater Lake caldera (Williams, 1942), Shikotsu caldera (Katsui, 1963), Aso caldera (Lipman, 1967), Katmai caldera (Curtis, 1968), Hakone caldera (Kuno, 1953), and Zavaritiski caldera (Gorshkov, 1970) suggest that the interaction of two distinct

magmas at shallow depth may be an integral part of the caldera-forming mechanism.

Many silicic magmas appear to have risen through the crust, and formed epizonal plutons such as the Tatoosh Pluton at Mount Rainier, Washington (Fiske et al., 1963), or erupted as lava flows with minor pyroclastics. A model for the formation of Crater Lake caldera must explain why the high-level dacite magma did not crystallize in place accompanied only by eruption of lava and cone-building ejecta. Instead, the entire zoned magma (approximately 60 km^3) was violently erupted as pyroclastic deposits of ash and scoria.

The Zoned Magma Chamber

The magma chamber which fed the culminating eruptions at Crater Lake contained two distinct magma types. Most of the erupted material was a uniform dacite equivalent to the earlier dacites erupted along the Northern Arc of Vents. Near the end of eruption, a more mafic magma was erupted as scoria flows. There appears to have been little or no intermediate material present. Final phases of eruption were characterized by expulsion of crystal-rich bombs of basic scoria and abundant fragments of andesite and granodiorite, and by rapid decrease in the energy of the eruption. Thus, it is concluded that a mafic magma occupied the base of the magma chamber in contact with granodiorite, and that eruption ceased due to depletion of

the magma chamber.

Fractionation of a uniform andesitic liquid to produce basic scoria accumulate and dacitic residual liquid is ruled out as a plausible mechanism for producing the zoned magma. Because Mazama andesite is intermediate in composition between the dacite and basic scoria magmas (Figure 4), and because the volume of dacite magma was approximately 70 km^3 , the volume of basic scoria magma that would result from such a fractionation process would also be approximately 70 km^3 . At most $4\text{-}5 \text{ km}^3$ of basic scoria magma can be accounted for in the deposits surrounding Crater Lake. Abrupt transition between the two distinct magmas is also inconsistent with fractionation of this type.

Crystal settling from a dacitic magma is ruled out as a plausible mechanism for producing the zoned magma. Again, abrupt transition between the two magma types is considered inconsistent with such a process. Also, the presence of fresh olivine in the basic scoria does not support such a mechanism.

Bulk chemical composition and presence of fresh olivine indicate that the basic scoria is related to contemporaneous parasitic eruptions of olivine-bearing basaltic andesite. Active assimilation of the granodiorite (which was in equilibrium with the dacite magma) by basic scoria magma indicates that this mafic magma was not in thermal equilibrium with the dacite magma. Therefore, the basic scoria

magma is considered to represent an injection of basaltic andesite magma into the base of the high-level crystallizing dacite magma chamber.

Development of hornblende in the basaltic andesite magma was a consequence of the abrupt change in equilibrium conditions experienced by the injected magma. A zone along the crystallized floor of the chamber was partially melted by contact with this hot mafic magma. The first mineral phases to be affected were the hydrous minerals (biotite and hornblende), and destruction of these hydrous phases released water to the invading magma. Increased water pressure produced by this assimilation promoted the stability of hornblende in the basaltic andesite magma, particularly near the bottom of the chamber where assimilation was most pronounced. Some hornblende grew around nuclei of olivine which were phenocrysts in the injected basaltic andesite magma.

Mechanism for Supersaturation of the Dacite Magma

High-level intrusion of a dacite magma beneath Mount Mazama was accompanied by tumescence and subsequent eruption along the Northern Arc of Vents. These eruptions were characterized by initial gas-charged explosions followed by extrusion of viscous lava. A considerable interval of quiet (4000-5000 years) followed the last

eruptions from the Northern Arc of Vents. Approximately 6600 years ago, eruption of dacite returned to Mount Mazama. There is no evidence that flank eruptions or extrusion of lava occurred at this time. These culminating eruptions were restricted to summit vents, and were characterized by highly gas-charged eruptions of pumice and scoria. Drastic changes in equilibrium conditions occurred in the magma chamber during the interval of quiescence. Somehow, the underlying magma developed sufficient gas pressure to initiate eruption. Once eruption began, gas-charged magma was violently expelled until the magma chamber was empty. The key to a caldera-forming model lies in the mechanism which would produce a rapid build up in vapor pressure within the magma chamber. This mechanism must develop gas nuclei throughout the magma (or at the base to be an effective driving force), so that once eruption begins, exhaustion of the magma is the only way to stop the eruption. Without a well-distributed gas phase, eruption would soon cease due to extrusion of viscous lava.

Crystallization of non-hydrous phases can increase the concentration of water in the liquid phase of a magma. Such a process must lead to increased water content of the magma, and perhaps to saturation with the resultant formation of a gas phase. At Crater Lake, crystallization may have saturated the magma with water. However, since crystallization at Crater Lake was slow, resulting

concentration of water and possible formation of a gas phase would be slow. Once a gas bubble formed, it could travel upward through the magma and escape from the system at a faster rate than crystallization could produce another equal volume of gas. Even if the roof of the magma reservoir was sealed, formation of hydrous crystalline phases, and increasing solubility of water in the liquid with decreasing temperature tend to retard a build up in vapor pressure within a cooling magma. Therefore, it is concluded that a simple cooling-crystallization model may saturate a magma with respect to water, but will not build up excessive vapor pressure within the magma chamber.

Williams and Goles (1968) suggest that withdrawal of a portion of the magma at depth may have triggered eruption. They do not explain in detail how such a mechanism would work. Presumably, subterranean withdrawal would initiate collapse of the summit, and in this way produce a low pressure exit for the magma. Reducing the external pressure below the vapor pressure of water in a particular magma can produce a gas phase. However, there is no evidence at Crater Lake for either withdrawal at depth or for pre-eruptive collapse of the summit. New data on Mazama ash volume indicate that there is no reason to assume a volume discrepancy between material erupted from the magma chamber and the volume missing from Mount Mazama. The radial distribution of glowing avalanche deposits around

the present caldera (Figure 3) suggests that eruptions came from central vents and not from fissures produced by collapse.

It is concluded that pressure release is a valid mechanism for mobilizing a magma. However, at Crater Lake increasing vapor pressure within the magma chamber appears to have exceeded the confining pressure and initiated eruption. Since subterranean withdrawal has been ruled out as a trigger mechanism, another mechanism must be developed which would produce a rapid build up in vapor pressure within the magma chamber.

Heating of a high-level, water-rich magma could lead to formation of a gas phase. If the magma were saturated at the time of heating, energy to provide the heat of solution necessary to develop a gas phase would be approximately 90 cal/gm (Goranson, 1931). Heating can be accomplished by uprise of an energy source in the form of a higher temperature magma. For example, a mafic magma near its liquidus could be 200-300°C hotter than a crystallizing silicic magma (Yoder and Tilley, 1962), and thus, a transfer of energy could occur. Crystallization in the heat source could theoretically maintain it at nearly constant temperature. Heat of crystallization (approximately 100 cal/gm) could then be transferred to the water-rich magma while a large driving force was still maintained. So, for every gram crystallized in the heat source, a gram of water vapor could be released in the cooler magma. Such a heating mechanism could

produce a rapid increase in vapor pressure which might then exceed the confining pressure and initiate eruption. Heat added to the bottom of the chamber would nucleate gas bubbles which would then rise toward the top of the chamber. By the time vapor pressure within the chamber exceeded the confining pressure, gas nuclei would be distributed throughout the magma. The largest gas bubbles would be found at the top of the chamber, and initial eruptions would be characterized by expulsion of fine ash and pumice. As the conduits increased in size, more magma would be erupted. Due to pressure release and transfer of heat from below, a level would be reached in the chamber where gas nucleation was active. Tiny gas nuclei distributed throughout the liquid would impart a fluidized character to the magma. At this point, magma would no longer be thrown high above the vent by expanding gas bubbles. Eruption would be characterized by glowing avalanches of fluidized magma, and would proceed until the gas-charged magma was exhausted.

A Summary of the Development of the Crater Lake Caldera

The eruptive products associated with Mount Mazama suggest that three distinct magma types were present. The first magma erupted throughout the region before, during, and after formation of Mount Mazama, and is recognized as olivine-bearing basaltic andesite. The second magma is hypersthene andesite and was restricted to flows

and minor pyroclastics which formed the main cone of Mount Mazama. The third magma was dacite which first appeared as flank eruptions of lava and pumice after the main andesitic cone had developed. Although these three magmas may have been genetically related at their depth of formation, they appear to have risen through the crust as independent bodies.

The following paragraphs review the sequence of geologic events that led to formation of the Crater Lake caldera. Special emphasis is placed upon the magmatic mechanism advanced above, and it is suggested that this mechanism may be a characteristic of all Krakatoan type eruptions. Specifically, they are produced when a high-level, water-rich magma is heated by the uprise of a higher temperature magma.

The main cone of Mount Mazama was built by eruption of hypersthene andesite. Shortly before the last major glaciation of Mount Mazama, eruption of dacite occurred along the south flank of the volcano. Following this first appearance of a silicic magma there is evidence of alternating eruptions of andesite and dacite. After the maximum glaciation of Mount Mazama, eruption of andesite and then dacite occurred along an arcuate fracture now marked by the north wall of the caldera. Eruption of dacite along the Northern Arc of Vents was a surface expression of the intrusion of a dacite magma at shallow depth beneath the volcano. Coeval with eruption of dacite along the

Northern Arc of Vents, parasitic cones of basaltic andesite developed on the lower slopes and plateau surrounding Mount Mazama. This mafic magma apparently was blocked from the central vents of the volcano by the presence of the high-level dacite magma body. The only evidence of mafic magma in or upon the main cone is the mixed mafic and siliceous cinders and lavas from Forgotten Crater. This occurrence may record a marginal encounter of ascending mafic magma with the high-level dacite.

Following eruption from the Northern Arc of Vents, glaciers readvanced over the Northern Arc lavas, and the dacite magma body appears to have reached a position approaching equilibrium. During this period of quiet, crystallization produced a solid rind of granodiorite around the magma chamber. Crystallization of plagioclase, hypersthene, and augite throughout the dacite magma increased the water content of the remaining liquid phase until a condition approaching saturation was reached.

The basaltic andesite magma which had previously erupted out on the flanks of the volcano now forced its way into the base of the dacite magma chamber. Injection of the basaltic andesite into this magma chamber may have triggered eruption of the composite lavas from Forgotten Chamber. At any rate, this magma was at a much higher temperature than the crystallizing, volatile-saturated dacite magma and its adjacent, crystallized rind. Assimilation of the

granodiorite floor of the magma chamber released water to the basaltic andesite. Due to increased water vapor pressure, hornblende became a stable phase in the injected magma, particularly near the floor of the chamber where assimilation was most pronounced. Hornblende crystallized as new phenocrysts and sometimes formed around the olivine nuclei which had been phenocrysts in the basaltic andesite.

Energy transferred from the high-temperature basaltic andesite provided the heat of solution necessary to release a gas phase in the volatile-saturated dacite magma. Gas nuclei formed near the base of the dacite, coalesced, and expanded as they traveled upward toward the top of the chamber. After a period of time, large bubbles were concentrated in the upper portions of the chamber with gas actively nucleating near the bottom. By the time vapor pressure within the magma exceeded the confining pressure on the chamber, a significant quantity of gas must have accumulated near the top of the system.

Eruption of dacite occurred several times at Mount Mazama, but never with the irreversible violence that characterized the culminating eruptions. Initially, the eruptions were highly gas-charged explosions. As the vents were widened and the high-level concentration of gas expelled, more and more magma was ejected as ash and pumice. After more than one-half the magma had been erupted, a level was reached at which gas was actively nucleating. The character of the eruption drastically changed, and no longer was the material thrown

high above the vents as disrupted liquid and gas phases. Tiny gas nuclei forming throughout the liquid caused the erupted magma to behave as a fluidized mass. Much of the material was erupted as glowing avalanches which swept down the slopes of the volcano and traveled for many kilometers across the surrounding plateau. That portion of the fluidized magma which was drifted away by the winds was much coarser than the earlier air-fall pumice. This appearance of fluidized magma is recorded as a discontinuity in particle size distribution in the air-fall deposits surrounding Crater Lake.

Violence of the culminating eruptions dropped sharply upon depletion of the dacitic portion of the magma chamber. The basaltic andesite magma which had triggered the eruption of dacite was itself expelled in the form of glowing avalanches. This unusual behavior of a mafic magma was made possible by the rapid decrease in pressure caused by expulsion of the overlying dacite magma, and aided by increased vapor pressure from assimilation of granodiorite. Eruption of basaltic andesite clearly marked the waning stages of the eruptive sequence which decreased in violence as deeper and more crystal-rich levels were tapped. Finally, the last dying eruptions deposited a thin chaotic layer of crystal-rich basic scoria containing granitic and andesitic fragments torn from the walls of the underlying chamber and conduits. These final products of the eruption indicate that the chamber had been exhausted of its eruptable magma. A sub-volcanic

vacancy of approximately 60 km^3 was produced. The unsupported summit of Mount Mazama collapsed into the void created by the preceding sequence of events, and the Crater Lake caldera was formed.

Mafic magma could now erupt through the central vents for the first time since the emplacement of the dacite chamber (approximately 5000 years before). Shortly after collapse, a lava lake of basaltic andesite formed on the floor of the caldera. At least two cinder cones grew on the caldera floor, and the last activity, represented by Wizard Island is chemically similar to andesite which formed the main cone of Mount Mazama. Thus, a violent cycle of volcanic activity had returned to its initial condition.

BIBLIOGRAPHY

- Baldwin, E. M. 1964. Geology of Oregon. 2nd ed. Ann Arbor, Michigan, Edwards Bros. 165 p.
- Blank, H. R., Jr. 1966. General features of the Bouger gravity field in southwestern Oregon. U.S. Geol. Survey, Prof. Paper 550-C. p. C113-C119.
- Chichester, F. W. 1967. Clay mineralogy and related chemical properties of soils formed on Mazama pumice. Ph. D. thesis. Corvallis, Oregon State University. 152 numb. leaves.
- Coats, R. R. 1968. Basaltic andesites. In: Basalts: the Poldervaart treatise on rocks of basaltic composition. Vol. 2, ed. by H. H. Hess and Arie Poldervaart. New York, Interscience. p. 689-736.
- Coombs, H. A. and A. P. Howard. 1960. Catalogue of the active volcanoes of the world including solfatara fields. Part IX. United States of America: International Volcanological Association, Largo, S. Marcellino 10, Napoli Italia. p. 1-68.
- Crandall, D. R. and D. R. Mullineaux. 1967. Volcanic hazards at Mount Rainier, Washington. U.S. Geol. Survey, Bulletin 1238. p. 1-26.
- Curtis, G. H. 1968. The stratigraphy of the ejecta from the 1912 eruption of Mount Katmai and Novarupta, Alaska. Geol. Soc. America Mem. 116. p. 153-210.
- David, P. P. 1970. Discovery of Mazama ash in Saskatchewan, Canada. Canadian Jour. Earth Sci. Vol. 7. p. 1579-1583.
- Diller, J. S. and H. B. Patton. 1902. The geology and petrography of Crater Lake National Park. U.S. Geol. Survey, Prof. Paper 3. p. 1-167.
- Easterbrook, D. J. 1969. Pleistocene chronology of the Puget lowland and San Juan Islands, Washington. Geol. Soc. America, Bulletin 80. p. 2273-2286.
- Fiske, R. S., C. A. Hopson and A. C. Waters. 1963. Geology of Mount Rainier National Park, Washington. U.S. Geol. Survey, Prof. Paper 444. p. 1-93.

- Garber, L. W. 1970. Influence of volcanic ash on the genesis and classification of two spodosols in Idaho. Masters thesis. Moscow, University of Idaho. 75 numb. leaves.
- Goranson, R. W. 1931. The solubility of water in granite magmas. American Jour. Sci. Vol. 22. p. 481-502.
- Gorshkov, G. S. 1970. Volcanism and the upper mantle. New York, Plenum Press. 385 p.
- Hamilton, D. L. and G. M. Anderson. 1968. Effects of water and oxygen pressures on the crystallization of basaltic magmas. In: Basalts: The Poldervaart treatise on rocks of basaltic composition. Vol. 1, ed by H. H. Hess and Arie Poldervaart. New York, Interscience. p. 445-482.
- Harward, M. E. and C. T. Youngberg. 1969. Soils from Mazama ash in Oregon: identification, distribution and properties. Pedology and quaternary research symposium, University of Alberta, Edmonton. p. 163-177.
- Jaeger, J. C. 1957. The temperature in the neighborhood of a cooling intrusive sheet. American Jour. Sci. Vol. 255. p. 306-318.
- King, P. B. 1958. Evolution of modern surface features of western North America. In: Zoogeography, ed. by C. L. Hubbs, Washington, D. C., American Association for the Advancement of Science. p. 3-60.
- Kuno, H. 1953. Formation of calderas and magmatic evolution. American Geophysical Union, Transactions. Vol. 34. p. 267-280.
- _____ 1960. High-alumina basalt. Jour. of Petrology. Vol. 1. p. 121-145.
- Larsen, E. S. 1945. Time required for the crystallization of the great batholiths of southern and lower California. American Jour. Sci. Vol. 243. p. 399-416.
- Lichti-Federovich, S. 1970. The pollen stratigraphy of a dated section of Late Pleistocene lake sediment from central Alberta. Canadian Jour. Earth Sci. Vol. 7. p. 938-945.

- Lipman, P. W. 1967. Mineral and chemical variations within an ash-flow sheet from Aso caldera, southwestern Japan. *Contr. Mineralogy and Petrology*. Vol. 16. p. 300-327.
- Macdonald, G. A. and T. Katsura. 1965. Eruption of Lassen Peak, Cascade Range, California in 1915: example of mixed magmas. *Geol. Soc. America, Bulletin* 76. p. 475-482.
- Matsuo, S. 1961. The behavior of volatiles in magma. *Jour. Earth Sci., Nagoya University*. Vol. 9. p. 101-113.
- McBirney, A. R. 1968. Compositional variations of the climactic eruptions of Mount Mazama. *Oregon Dept. Geology and Mineral Ind., Bulletin* 62. p. 53-56.
- Noble, D. C., J. C. Drake and M. K. Whallon. 1969. Some preliminary observations on compositional variations within the pumice- and scoria-flow deposits of Mount Mazama. *Oregon Dept. Geology and Mineral Ind., Bulletin* 65. p. 159-164.
- Peacock, M. A. 1931. Classification of igneous rocks. *Jour. Geology*. Vol. 39. p. 54-67.
- Peck, D. L. *et al.* 1964. Geology of the central and northern parts of the Western Cascade Range in Oregon. *U.S. Geol. Survey, Prof. Paper* 449. p. 1-56.
- Rai, D. 1971. Stratigraphy and genesis of soils from volcanic ash in the Blue Mountains of Eastern Oregon. Ph. D. thesis. Corvallis, Oregon State University. 136 numb. leaves.
- Shimazu, Y. 1960. Physical conditions of contamination and fractionation of basaltic parental magmas. *Jour. Earth Sci., Nagoya University*. Vol. 8. p. 72-85.
- Taylor, E. M. 1967. Accidental plutonic ejecta at Crater Lake, Oregon. *Geol. Soc. America Ann. Mtg.* p. 221. (Abstract)
- Turner, F. J. and J. Verhoogen. 1960. *Igneous and metamorphic petrology*. 2nd ed. New York, McGraw-Hill. 694 p.
- Westgate, J. A. and A. Dreimanis. 1967. Volcanic ash layers of recent age at Banff National Park, Alberta, Canada. *Canadian Jour. Earth Sci.* Vol. 4. p. 155-161.

- Williams, H. 1942. The geology of Crater Lake National Park, Oregon. Carnegie Institute of Washington. Publication no. 540. p. 1-162.
- _____ 1961. The floor of Crater Lake, Oregon. American Jour. Sci. Vol. 259. p. 81-83.
- Williams, H. and G. G. Goles. 1968. Volume of Mazama ash fall and the origin of Crater Lake caldera. Oregon Dept. Geol. and Mineral Ind., Bulletin 62. p. 37-41.
- Williams, H. and A. R. McBirney. 1968. Geologic and geophysical features of calderas. NASA Progress Report CR-93188. p. 1-87.
- Wise, D. U. 1963. An outrageous hypothesis for the tectonic pattern of the North American Cordillera. Geol. Soc. America, Bulletin 74. p. 357-362.
- Yoder, H. S. and C. E. Tilley. 1962. Origin of basalt magmas: an experimental study of natural and synthetic rock systems. Jour. Petrology. Vol. 3. p. 342-532.
- Youngberg, C. T. and C. T. Dyrness. 1964. Some physical and chemical properties of pumice soils in Oregon. Soil Science. Vol. 97. p. 391-399.